Clear Active Contact Lens
(CACL)

Senor Project Report

Advisor:
Dr. Smilkstein
Multidisciplinary Preparees:
BMED BS - Paul Hecker (pheckler@calpoly.edu)
BMED BS - Phillip Azar (pazar@calpoly.edu)
EE BS - Alexander Do (ado03@calpoly.edu)
EE 4+1 – Benny Ng (beng@calpoly.edu)
EE 4+1- Errol Leon (ehleon@calpoly.edu)

Table of Contents

I Abstract

The clear active contact lens project aims to address safety and hazard awareness with an unexplored field of eye wear technology. With advancements in nanotechnology and the advent of circuits on contact lens, this project is one of the first research and development into this new field, following University of Washington and Google. The team focuses on the safety and biocompatibility of the contact lens for a comfortable ease of use. The designs push the limits of thin film printed technology with its pursuit of fine designs of 250μm antennas. The project streamlines the manufacturing process for a combination substrate of PET and PDMS and mounting of antenna, IC, and battery. To produce a product that operates at simulated specifications, the team tests and characterize the substrate, antenna, IC, and battery separately, while ensuring their designs function effectively together. The designs and processes provide a large stepping stone to the realization of a marketable active contact lens.

II Introduction

In today's working world, a significant amount of attention is placed upon occupational health and safety. In the United States, a section of the U.S. Department of Labor known as the Occupational Health and Safety Administration (OHSA) proposes, manages, and enforces laws detailing safety requirements in the workplace. These efforts have contributed to an overall decrease of 7% in occupational fatality rates from 2011 to 2012 [1]. The clear active contact lens project is an effort to continue to improve the safety and quality of life of hazardous environmental workers by providing them an internal means of awareness in unsafe situations. The project also seeks to build on already available technology in designing active contact lenses and improve on them with thinner integrated circuitry, more robust battery design, and wireless inductive charging.

In a hazardous environment, an individual's awareness of risk factors is critically important to their safety. In many situations, these risk factors are invisible to our senses, such as radiation or odorless fumes. The individual must rely on external equipment to provide them with the information needed to complete their task and keep themselves safe. This equipment can be large, cumbersome, and in some cases (such as Geiger counters) outdated. The project aims to facilitate this provision of information by changing the means of delivery. Rather than an individual having to process the information provided to them by external equipment, the individual will be able to react to information provided immediately through a small, unobtrusive device that can be integrated internally. The device will rely on sensory circuitry to process the information for the user, and when harmful conditions are detected, deliver a sensory stimulus, such as a flashing light or audio message. Through proper training, this quick reflex can help the user remove themselves from a dangerous situation much more rapidly and effectively, and thus lower incidence of injury.

The Clear Active Contact Lens project began as an interdisciplinary effort, and after

being awarded the CP connect interdisciplinary project grant in winter of 2014, was realized in the spring of 2014. Final prototypes were also delivered as a fulfillment of the arrangement set in biomedical engineering design. Motivation for the project lies within each individual group members commitment to building devices that contribute to the wellbeing of others, and financial incentive in the project are a result of a relatively premature market ripe for research and development.

III Background

The foundation for this project was set by research conducted at University of Washington by Otis *et al.* [2]. In their research, a proof-of-concept active contact lens powered by radio frequency waves was developed and tested. This research demonstrated the feasibility of a small-form factor application of an integrated device within a contact lens, and can be seen below in Figure 1.

Figure III-1: Radio frequency powered contact lens. Left side shows unlit LED, right side shows LED when lit. [1]

Contacts are one of the few disposable devices that come into direct contact with the interior of the body for extended periods of time [4]. A lens equipped with the proper detection facilities could continuously measure biomarkers present on the surface of the eye. Many of these biomarkers are likely the same ones analyzed by doctors following a blood test, meaning that this device could provide a less invasive form of measurement and provide patients with a more continuous stream of data. Early implementations of this concept can be seen in devices that have been designed to measure glucose concentrations in tear solution, and were built using micro fabrication and silk-screen deposition processes [2]–[4].

The device does not need to be complicated to provide functionality [2]. By designing the device so that it responds to external stimulus, much of the hardware associated with processing and detection can be offloaded, while maintaining the benefits of an ocular indication system. To our knowledge, no one has shown a fully integrated device that is capable of powering an onboard LED in response to external stimulus.

Up until this point as well, biocompatibility has largely been neglected in the quest for a working device. Babak *et al.* partially acknowledged this concern by coating their device in a biocompatible substance known as parylene. However, parylene has a significant downside for ocular implementation, as it is impermeable to oxygen, which is necessary for proper functioning of the cornea. [8] In addition to biochemical concerns, effects of heat dissipated by the battery, circuitry, and antennae will have to be taken into account when determining the safety of the device. Since the device is electromagnetic in nature, it will have to comply with a wide variety of standards governed by different regulatory bodies including the FCC and FDA [9].

IV Customer Requirements and Design Requirements

The goal of this project is to create a prototype that can prove the efficacy of an active contact lens. In our design process this year, we identified a number of customer requirements that are most important in the usage of the device, and translated them into engineering specifications. The first requirement we could gather was that the lens needed to be clear. Our initial target customer base is largely situated in hazardous waste control. In this occupation, unclouded vision is absolutely necessary. The individual must be completely aware of what is in front of them and around them through the use of visual recognition, since environmental suits will obstruct other senses, such as smell, hearing, and touch. Another requirement is comfortability, since the individual will more than likely not be able to perform any field adjustments on the lens itself. This is by far one of the most difficult requirements to incorporate into device design. As such, any materials used will need to be inspected for minimal adverse reactions, with the most important being inflammation, when in contact with the body. Finally, the terminal requirement is isolated functionality. To remain competitive in the young market place of active wearable devices, the clear active contact lens must not require any input or command from the customer. The device must maintain autonomy from the user so that he or she can focus on the task at hand. When the device has meaningful data to provide, it will do so with a designated stimulus, in our case an LED. Otherwise, it will remain off and out of the way.

In developing accurate engineering specifications, the clear active contact lens project group opted to split the device into separate categories of requirements that are interlinked: material properties and electrical properties. An updated design table of design requirements has also been included in the appendix for reference.

Material Properties

Clearness

The clearness of the lens is largely governed by the material used to fabricate the lens, as well as any surface coating applied to the lens surface. The refractive index of a material, n_D, is a dimensionless number that describes how light and other radiation propagates through a material. It is obtained by the following equation, which divides the speed of light in a vacuum by the speed of light in a substance:

$$n = \frac{c}{v} \qquad \text{(EQ 1)}$$

Since the prototype will not be a prescription lens, a best fit material would have a refractive index close to 1, meaning that light entering through the lens would be refracted a very small amount, and the individuals vision would not be blurred significantly. This, along with biocompatibility and flexibility, will govern the materials selection process in our project. It is important to note that achieving a refractive index of 1 with commercial polymers is unlikely. Commercially available polymers have refractive indices that range between 1.3 and 1.7. [10] As such, we have determined that a refractive index between 1 and 1.5 will be acceptable for our application. This range of indices is acceptable because the eye itself will refract light based on a desired level of acuity. If the refractive index is within the range we have specified, the eye should be able to distinguish objects without any loss of acuity.

Also in the way of clearness is the placement of any circuitry on the lens. In the current design, the pupil area of the lens must be free of any and all obstruction by circuitry. This includes up to 9 mm in diameter of obstruction-free material. Any circuitry on the lens must be clear circuitry, or be such that the eye will not be able to resolve the obstructing items at any time.

Flexibility

The next requirement that will largely impact the design is flexibility. The defining aspect of this project is the development of a contact lens. As such, any material chosen to support that design must be able to flex to the curvature of the surface of the eye, and in doing so not incur significant stress as to damage the lens itself. The method of quantifying flexibility relies on the computation of the stiffness, k, of the material. This is given in relationship to the young's modulus, E, by the following equation:

$$k = \frac{AE}{L} \qquad \text{(EQ 2)}$$

Where A is the cross sectional area of the sample and L is the length of the sample. In general, the higher the value of k, the stiffer the material becomes. In materials selection, this means that the higher the young's modulus of the material, the stiffer it becomes per element. However, the lower k is, i.e. the more flexible the material is per element, and the lower the young's modulus becomes. A material with too low a young's modulus can be at a higher risk of plastic deformation, and in the worst case, failure. Failure in this category is defined by exceeding the ultimate tensile strength of the material and resulting fast fracture. It is important to note that the above equation represents axial stiffness. In the current problem, generalizations regarding the bending of the lens as a two dimensional stiffness problem can be

made by assuming young's modulus is isotropic for the contact lens.

The target for flexibility is measured directly by Young's modulus, E, of the material chosen. A large range of these values are listed in table III in the appendix. This variance is a result of the two top material candidates having opposite flexibility, with PDMS being relatively compliable compared to PET.

Another factor which is directly impacted by flexibility is the integrity of any onboard circuitry. The circuitry must be able to bend without incurring significant damage or wear. The device will be tensile tested before and after circuitry is laid on, so as to characterize the mechanical durability of the device.

Biocompatibility

A staple of biomedical design is the process of determining the suitability of a material in a medical device application. This means that the material must not do harm to the body within the intended function, and the body must not do harm to the material. This is by far the most difficult requirement to contend with from an engineering perspective because it does not have a quantifiable nature. Instead, biocompatibility analysis is performed during acute and chronic studies on cells, living systems, and even live patients. The data from these studies is then compiled and analyzed by a team of biomedical engineers, who look at notable examples of bioactivity such as inflammation, systemic toxicity, and rejection. Since the product will be in direct contact with the user's eye for the duration of their task, any material selected as the base for the lens must not be sufficiently biocompatible.

Many commercial polymers used in the biomedical industry have already been characterized for biocompatibility. This, however, can be a double edged sword. This data may not be for the region of interest, i.e. the surface of the eye. Also, this data can limit the materials selection process significantly, to the point where a suitable material may not currently exist. As such, determining a material from the perspective of biocompatibility is a peripheral effort: it is impossible perform studies with resources currently available. A reliance on currently available data will be the primary means of analysis of biocompatibility.

Currently, both PET and PDMS are characterized as relatively biocompatible, with the former being a known irritant due to its relatively low oxygen permeability when compared to PDMS. PDMS stands currently as the best material for biocompatibility when in contact with the eye, as many modern contact lenses utilize PDMS as a substrate material. What this means for the clear active contact lens project is substantial: the usage of a PDMS substrate would significantly strengthen the pursuit of a 510(k) clearance with the FDA.

Electrical Requirements

Size

Size is an important parameter for the design of any electrical components on the electronic side of the lens. The contact lens itself is very small, with a maximum surface area of .8 cm^2. No circuitry will be allowed in the area bound by the pupil, thus further decreasing the area available for electronic components. The resulting size budget changes the method in which the project will approach manufacturability of the lens itself. The small size also directly impacts the functionality, which will be limited by the physical constraints associated with small circuits [11]. Micro fabrication is a likely route to remedy this issue, since printed circuitry may result in critical conductor discontinuities. This, in turn, would create a non-functional device.

Determining what is too big and what is too small will come directly from the cost and relative need of both. Since the electrical components of our design include an integrated circuit, an antenna, and a battery, the budgeting will be dependent on the importance of the component and the cost required to manufacture at that size. As of early March, the clear active contact lens electrical size budget will include a narrow strip revolving around the eye equivalent to the difference of the total area and the maximum pupil dilation area. Further technical information regarding constraints specified by the client can be seen in the Appendix under IC Design and Antennae.

Power and Heat

Modern electronics run largely on AC dynamics, and as such, power generated and used by a circuit will consist of two components: real power and imaginary power. From a systems perspective, the power that has the potential to be dissipated as heat comes in the form of real power, given by the following equation:

$$P = \frac{1}{2} V_p I_p \cos\theta = V_{rms} I_{rms} \cos\theta \qquad \text{(EQ 3)}$$

Where V_{rms} represent root mean square voltage, I_{rms} represents root mean square current, and θ represents the phase angle. This power is in units of Watts, and is consumed by the system in question. Calculations can be done after obtaining real power to determine the heat dissipated within a specific timeframe of use, by multiplying the real power by the total active time. In our design, the active portion of the contact lens must generate and use a little power as possible, due to the danger of excess heating in the eye and electrical safety. Comfortability of the user will directly depend on how hot the circuitry becomes.

In the project, it will be assumed that the system will not become hot enough to damage the onboard circuitry (i.e. temperatures above 60 degrees Celsius.) COMSOL simulations performed indicated that given the maximum power output of 10 mW. In this regard, maximum allowed change in temperature is given as 1.5 degrees Celsius, and will be tested with PET, PDMS, and combination lens models.

Functionality

The device's functionality will be the primary determinant of the efficacy of the overall product. If the device cannot provide a degree of functionality that will alert the user to hazardous environmental conditions based on a preset threshold, then the device will fail to meet FDA efficacy requirements. The device also has to improve in some way on past iterations of active contact lenses. This requirement is largely accounted for by the concept of isolated functionality, in which the device requires no interaction from the user besides putting the contact lens on properly to perform within specified limits.

This requirement necessitates the creation of an external component that communicates with the contact lens itself. Sensory circuitry is too large to fit in the budgeted area of the contact lens, and must be placed off board. This off board circuitry will be contained within a small device on the user in order to process any information collected by the onboard integrated circuitry. The antenna will provide a means of communication between the two circuits, and effectively "link" them. Antenna design and verification is largely based on the mode of communication used, in this case, the IEEE 2.4 GHz band. The radiative resistance must be high enough to send and receive signals, and the inductance must be such that wireless inductive charging is permissible. A spectrum analyzer will be sufficient to test the radiofrequency properties of the antenna, whereas simulations must be used to determine the inductance of the proposed antenna design prior to manufacture.

V Design Development

Concept Generation

Indicating danger to a user in a low foot-print setting allows for a wide variety of solutions. Any of the five senses could be stimulated to indicate danger. To narrow down the options we limited it to sight and touch, as these sense could be easily stimulated with technologies we had experience with. From here, we decided to focus on the eye. Our sponsor had a strong desire to make the project medically oriented, and since the eye is one of the most unique sources of biometric information that can be obtained noninvasively, we decided to focus our efforts there.

Once a focus had been established on the eye, the question became whether to use a external framework or an on-eye solution such as a contact lens. Products such as a google glass already existed, so we looked into how we could capitalize upon this to provide active functionality. It was soon apparent however, that while google glass was an incredible technology, it was more obtrusive and was designed for much more complex interaction than we required. The focus then shifted towards contact lenses.

Our group had limited experience with active contact lenses, but healthy imaginations. We drew on fantastical ideas such as x-ray vision to more realistic lenses that changed the color of the eye. With ideas such as this in mind, we went forth and did a comprehensive literature review. Here we found a small but blossoming field of active contact lenses. These lenses changed color in response to tear glucose levels, measured the pressure of the eye, and could receive wireless signals that activated LED's on the lens [5]. While many of these lenses were impressive in concept, a major challenge that had not been overcome was transporting data from lenses externally without the use of wires.

This challenge seemed beyond the scope of the project, so we instead focused our efforts on making a lens that had an on-board power source and could actively respond to indicated danger to users. This would allow us to create a fully functional device that could operate in conditions, such as inside a helmet or during sports, that a more external device such as google glass could not. It also allowed us to take one step closer towards a fully functioning biosensor by acting as a proof of concept for a fully-functioning embedded lens system, something which has never been done before and also met our sponsors desire to keep the project medically oriented. With this path in mind, we began translating our general concept into more concrete designs that would fulfill our design requirements.

Top Concepts

Since the clear active contact lens project was a heavily interdisciplinary, the three top concepts listed below largely represent the physical parameters of the lens. Each individual component, including the antenna, battery, integrated circuit, substrate material, and indicator, will fit into any of these designs. Rather than discuss the heavily iterative and rapidly changing design process for each individual component, we will focus more on discussing the implications of each component and the analysis performed to assist in the decision making process.

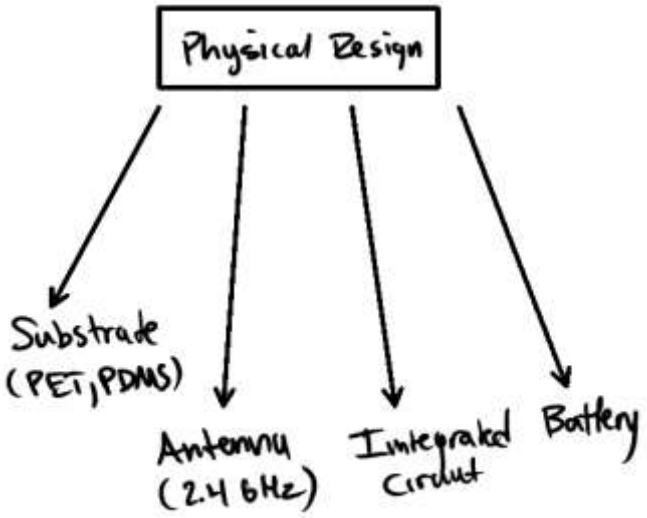

Figure 1: Map illustrating component connection to physical design.

1.25 cm Contact Lens - PET Substrate - RF Scavenging

The original design of the active contact lens was that of a typical contact lens, with a 1.25 cm diameter. The RF antenna would be laid onto the substrates around the rim until the proper inductance was reached for wireless charging. The differentiating factor of this lens, however, is that it would have to primarily rely on RF scavenging to recharge the battery, as the current tests indicate an inductance too small to support wireless charging at 2.4 GHz. Then, the integrated circuitry and thin-film battery would be placed parallel to the LED at the center of the lens, connected by conductive tracing ink. A layout sketch of this design is shown in figure V-2 on the next page.

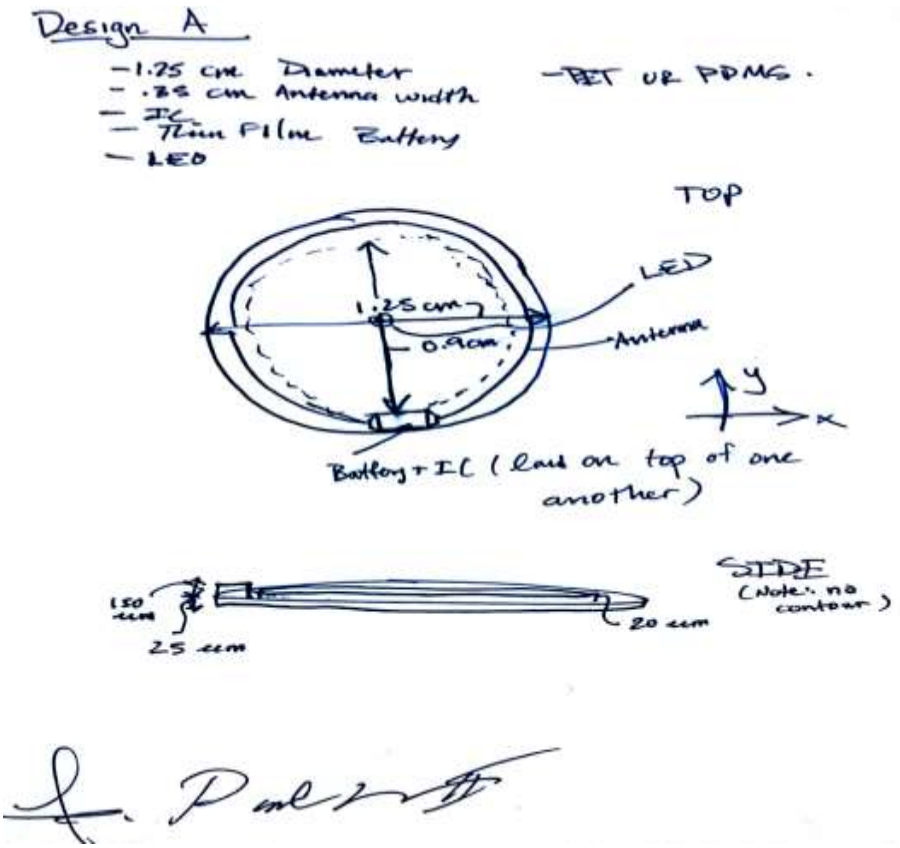

Figure 2: Layout sketch for 1.25 cm diameter lens design.

What is distinct about this design is that it was originally intended to be an all PET lens, following suit with work done at the University of Washington. PET is not only very easy to obtain in very thin sheets (~25 microns per sheet,) but it is also readily compliable when heated to 180 degrees Celsius, allowing for an easy curving process. Another benefit of PET is that the antenna can be printed directly on using a screen printer, simplifying the manufacturing process immensely. At first glance PET seems like the right choice for hosting a functional platform on a contact lens. PET, however, is not a comfortable material. It is traditionally considered a “hard” lens material and has a rough surface similar to paper. Also, after it has been curved, it has a tendency to crumple like paper around the edges, damaging the edge of the device and potentially preventing proper usage.

2 cm Contact Lens - PDMS Substrate - Wireless Charging

A newer design that takes cues from scleral lenses was conceived to produce better inductance for the wireless charging capabilities of the lens. The differences in this design and the previous include the type of substrate, the size and number of turns of the antenna (which correlate directly to inductance,) and the placement of the battery and integrated circuitry. A layout sketch is shown in figure 3 on the next page.

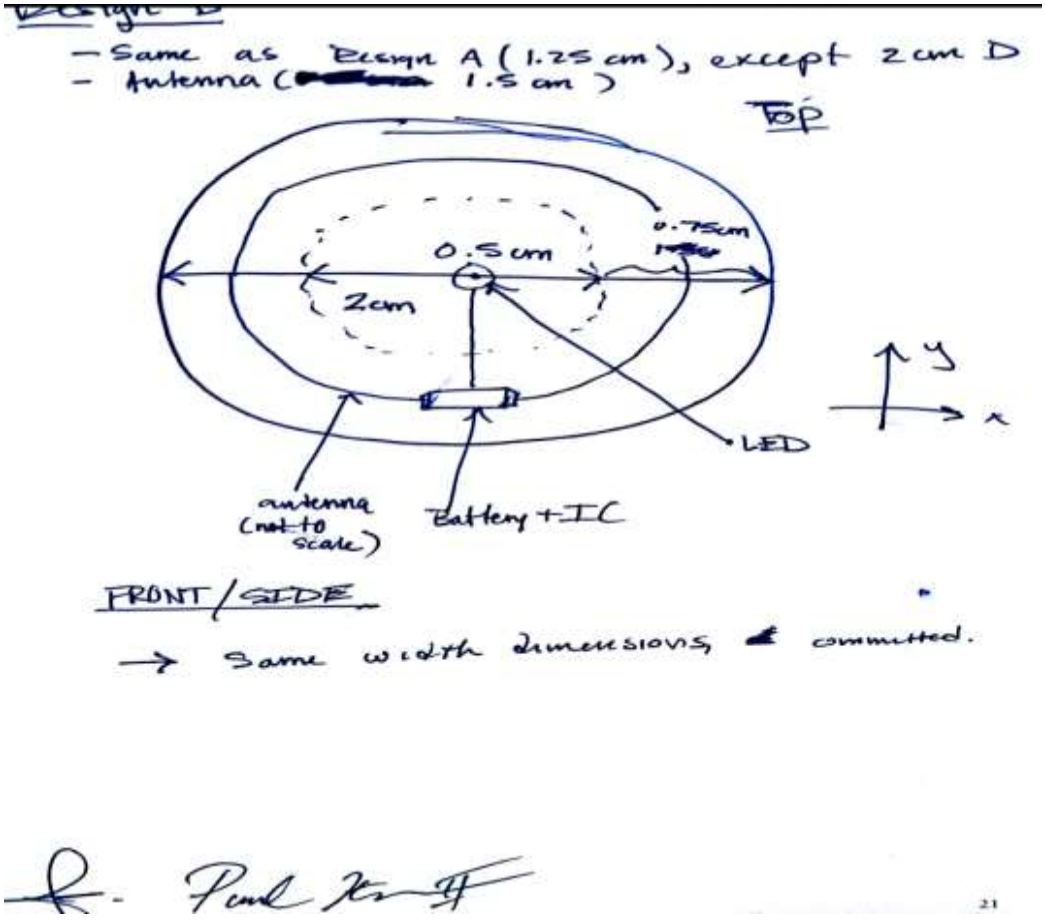

Figure 3: Layout sketch for 2 cm diameter lens design.

While this lens is clearly much larger, its conception was largely a result of a large quantity of simulation performed on both electromagnetic and thermal properties. The larger lens allows for the implementation of a much more powerful wireless platform that can both charge the embedded battery and receive incoming RF signals. This lens also is completely constructed of PDMS, a material well characterized for application where *in vitro* and *in vivo* biocompatibility is a major factor.

When our team evaluated this idea, we came to the consensus that while it solves many of the problems of the 1.25 cm design, it comes with a host of manufacturing challenges. The first is that in order to make a full PDMS lens, the entire process must be done in a micro fabrication space. This means that actually generating a prototype will expensive, arduous, and relatively temperamental. Additionally, a number of the resources needed to make an all PDMS design work are restricted to micro fabrication trained individuals. This means that much of the development of a proposed prototype would have to be supervised, which could potentially further slow the development process.

1.5 cm Contact Lens - PDMS Exterior, PET Interior - Wireless Charging

The final design concept our team generated was a fusion of the previous two designs, and an appropriate middle ground. With a proposed 1.5 cm diameter, wireless charging, and dual composition, the 1.5 cm lens represented the strongest and most feasible candidate for a prototype in our design process. The caveats, however, were apparent from the start. The lens would have to be manufactured in many more steps than previous iterations. Instead of a two or three step process, we now had a five step process over many hours. Also, since this lens design had effectively three layers, the risk of air gaps and material separation was much higher. A sketch of this design can be seen in figure 4.

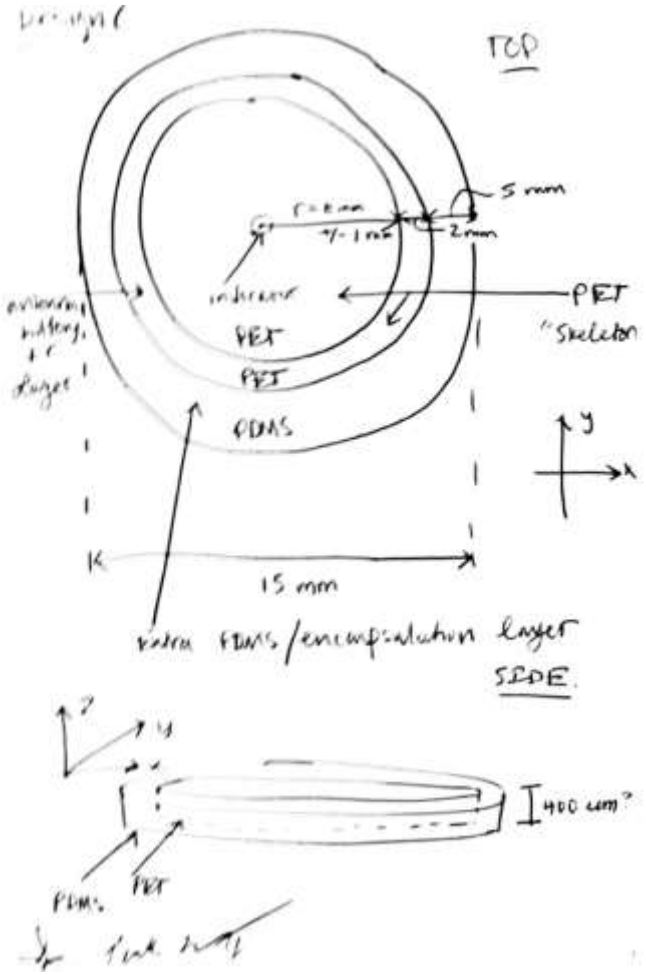

Figure V-4: Layout sketch for 2 cm diameter lens design.

Preliminary Analysis - Design Selection Process

The selection process was broken into three stages: functional requirements, manufacturing requirements, and cost limitations.

Functional

The first stage focused on meeting the functional requirements. This required that the device meet the material and electrical properties specified in the design requirements, in addition to achieving its overall goal of operating as a warning indicator embedded in an active contact lens. Functional requirements were extensively tested to determine the overall direction of the project. The five major areas of concern included power dissipation and bioheat transfer, antennae design, battery design, integrated circuit design, and safety concerns.

Power Dissipation and Bioheat Transfer - COMSOL Simulations

The goal of simulations performed this quarter was to characterize the thermal effects of the active contact lens on the human eye for prolonged periods of time. Simulations were performed with both candidate substrates, PET and PDMS, and circuitry was simulated as a constant power source. Bioheat transfer analysis based upon the Pennes bioheat equation was performed in COMSOL with a close approximation of the finite element model proposed by Gokul K.C. *et al.* [12]

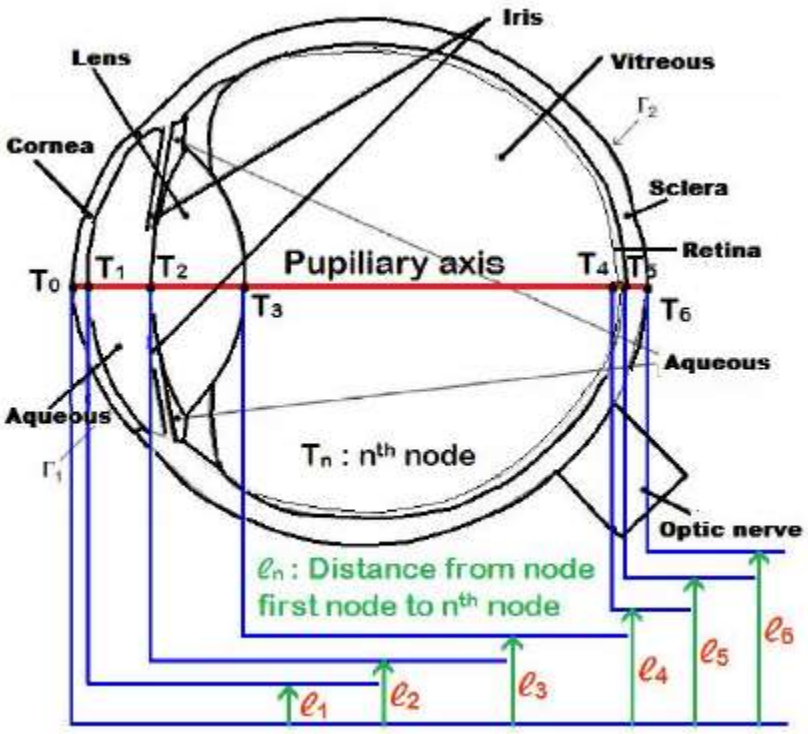

Figure 5: Proposed finite element sketch of Human eye.

Where T0 through T6 represent nodal temperatures up to the *n*th element of the model, and L1

through L6 represent distances from the surface of the cornea to the *n*th element of the model. The above model was used primarily as a reference in which to approximate our simplified model, seen below:

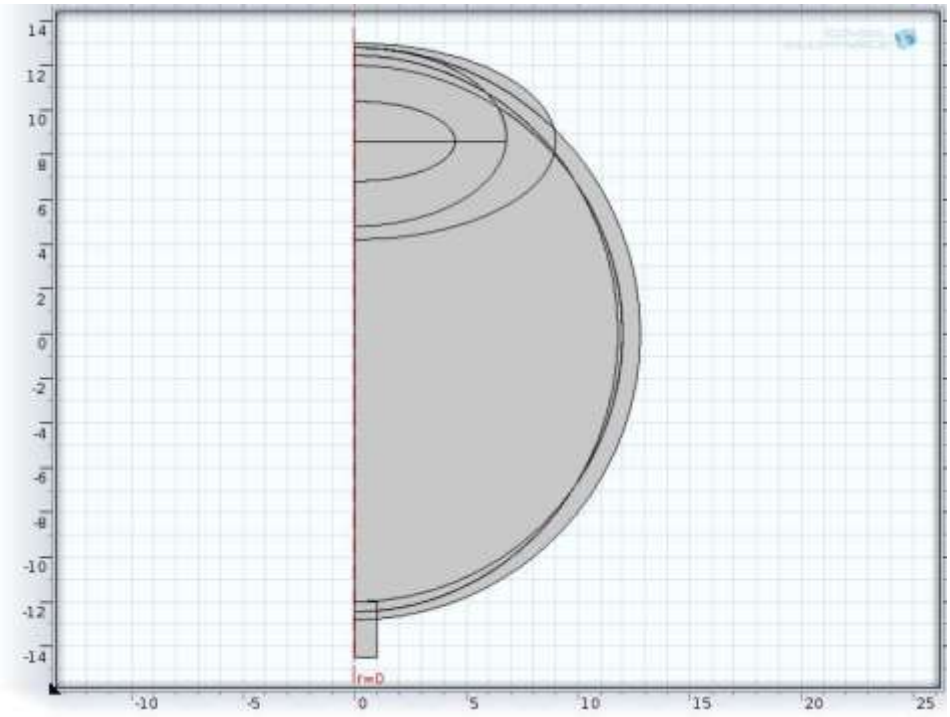

Figure 6: 2D Axisymmetric COMSOL sketch of the human eye.

The above model was simplified significantly primarily to reduce computational time required in COMSOL and to reduce complexity of the resulting temperature distribution. Also, it can be seen that at the top of the model, around r = 12 mm, we have included an approximation of the contact lens, with a varying thickness of 250 to 400 micrometers. The thickness is such that at the center, it is smallest, and at the edges, it is largest. This variance was designed in order to remove the need for a complex Bezier polygon geometry when simulating the contact lens in COMSOL.

In our model, we assumed that the temperature of the surface of the cornea was 35 degrees Celsius, 2 degrees Celsius lower than the rest of the eye. There are two primary reasons for this assumption. First, convective heat flux at the surface of the eye associated with tear flow and gas flow naturally reduce the surface temperature of the cornea. Second, surface to ambient radiation will further reduce the temperature of the surface of the eye as temperature increases. Blood perfusion rates within the ciliary body and retina and various thermal properties of the eye were extracted from works by Gokul K.C. *et al.* and Cvetkovic *et al.* [13]

Using a 10 mW total power dissipated by the contact lens, the following temperature distributions were obtained from a time dependent simulation with 180 second end time and 0.1 second step size for both PET and PDMS:

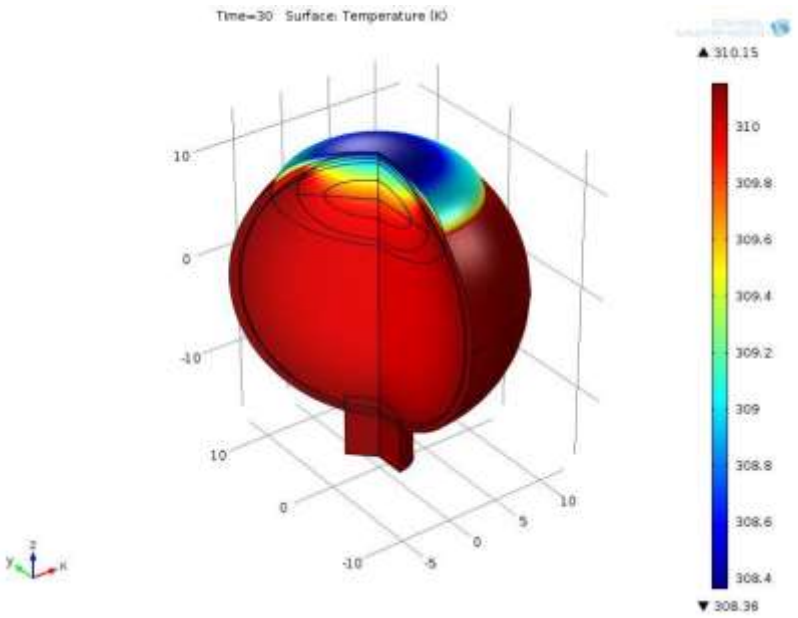

Figure 7: 3D surface temperature distribution after 30 second exposure - PDMS

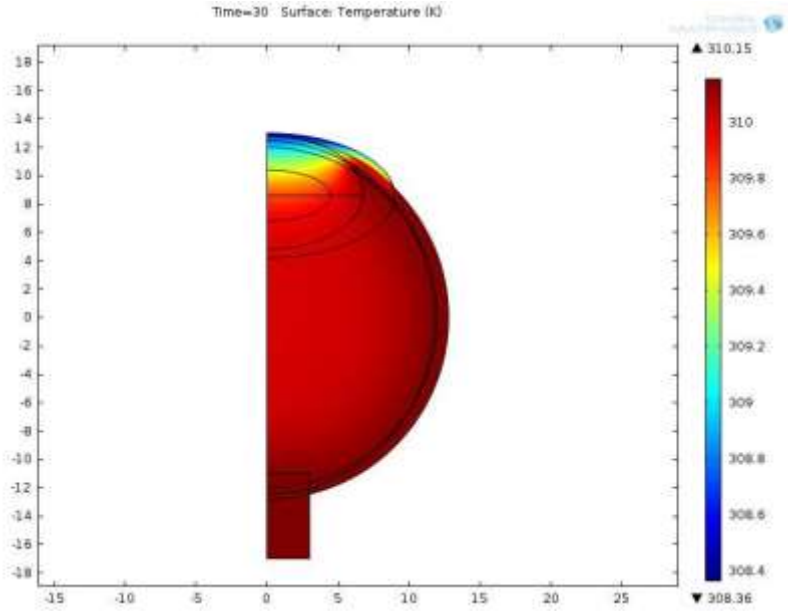

Figure 8: 2D surface temperature distribution after 30 second exposure - PDMS

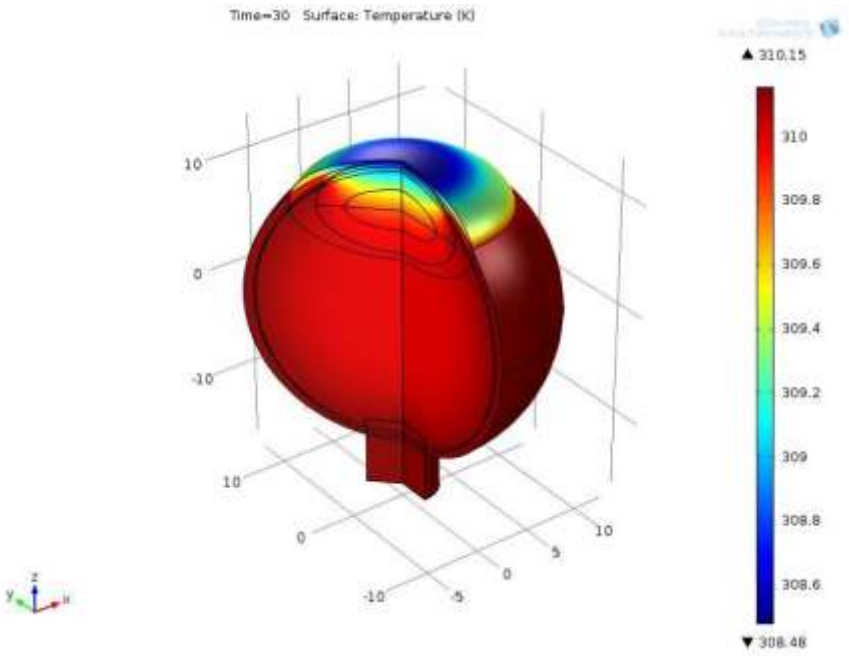

Figure 9: 3D temperature distribution after 30 second exposure - PET

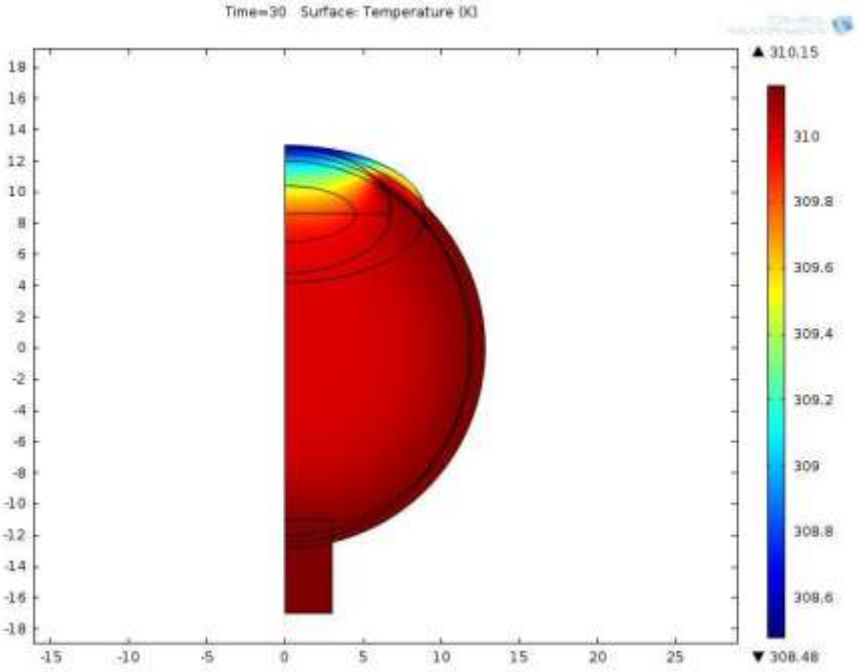

Figure 10: 2D surface temperature distribution after 30 second exposure - PET

For the simulations shown above, PET has a thermal conductivity of 0.24 W/m*K, a density of 1380 kg/m^3, and a specific heat capacity at constant pressure of 1000 J/kg*K. PDMS has a thermal conductivity of 0.15 W/m*K, a density of 970 kg/m^3, and a specific heat capacity

at constant pressure of 1460 J/kg*K. What can be determined from the above results is that PDMS is more thermally insulative than PET, and when exposed to the same conditions, causes a higher average temperature throughout the cornea. The gravity of this difference, however, is quite small. The values are within 0.005 degrees Celsius of each other. More importantly, however, is that the above bioheat simulations indicate that even at our maximum allowable power dissipation, the temperature change throughout the cornea is very small, ranging from a 0.5 to 0.7 degrees Celsius increase in both cases. From this it was concluded that from a bioheat transfer perspective, both substrates were equivalent and therefore the size is irrelevant, and the power budget for the onboard circuitry was appropriate.

Radiofrequency Engineering - Antenna design and Inductance

The primary goal of radio frequency engineering performed this quarter was to characterize the efficacy of the antenna as not only a receiver component of the active contact lens, but also as an inductive coil capable of charging the onboard battery. Since all components are largely immovable following manufacturing, without proper inductance from the antenna, sufficient power transfer will not be achieved, and the active contact lens will be a one use product. Since a nearly five thousand dollar disposable contact lens has no real market, the antenna is a crucial aspect of the project.

Three different antenna designs were investigated when selecting an overall design for the project. The first design, shown in figure 11, consisted of a continuous loop antenna of uniform trace width. This antenna was conceived under the assumption that the antenna could double as both an inductive coil and signal receiver. The second design, shown in figure 12 on the next page, attempts to improve efficiency at 2.4 GHz by adding an inner coupling loop. The third design, shown in figure 13 on the next page, is an adaptation of an antenna designed by Steve Yates that uses a small inner loop to improve efficiency at 2.4 GHz.

N (turns)	8
D_i (inner diameter)	7885um
D_o (outer diameter)	11630um
W (trace width)	117um
S (trace spacing)	117um

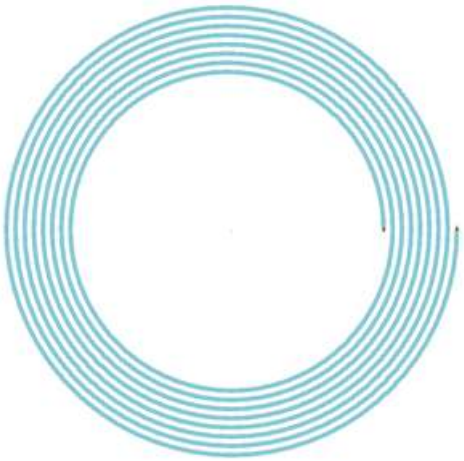

Figure 11: First antenna design, consisting of one solid loop of uniform trace width.

This was the first design with the assumption that we can use the inductive coil as the antenna. In order to fit the outer diameter size constraint, we were not able to use a λ/3 design,

so we used a 7λ/24 circumference, which has an 11.63mm outer diameter. This gives better efficiency than λ/4 while remaining under 12mm diameter. This coil has 8 turns with an inner diameter of 7.885mm, which is only 1.5% less than our inner diameter requirement. Out of our 3 designs, this had the highest inductance, but severely lacked power efficiency at 2.4GHz. Our simulation gave us an antenna gain of -22.3dB at 2.4GHz, which was the lowest of our designs. Using Harold A. Wheeler approximations for planar coils operating under 30MHz ($L(\mu H) = \frac{D_o^2 \times A^2}{30 \times (A-11) \times D_i}, A = \frac{D_i + N(W+S)}{2}$), we calculated the inductance to be 1.005μH. This design is by far the best for inductive charging.

Antenna Ring	diameter	11900um
Antenna Ring	trace width	500um
Antenna Ring	trace spacing	103.5um
Inner coil	N (turns)	1.605
Inner coil	D_i (inner diameter)	8000um
Inner coil	D_o (outer diameter)	9262.7um
Inner coil	W (trace width)	250um
Inner coil	S (trace spacing)	250um

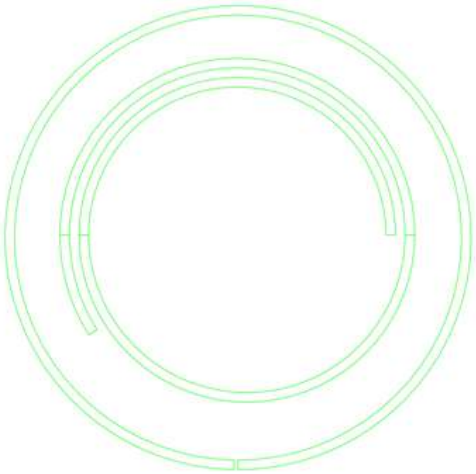

Figure 12: Second antenna design, consisting of two separate loops of uniform trace width.

This second design makes use of a large trace antenna outer loop and a 1.6 turn inner coupling coil to achieve a gain of -14.5dB at 2.4GHz. This greatly improved gain sacrifices inductance of 20nH, which is based on the minimal windings of the inner coil. This was able to almost double its power efficiency by doubling the trace width of the antenna coil.

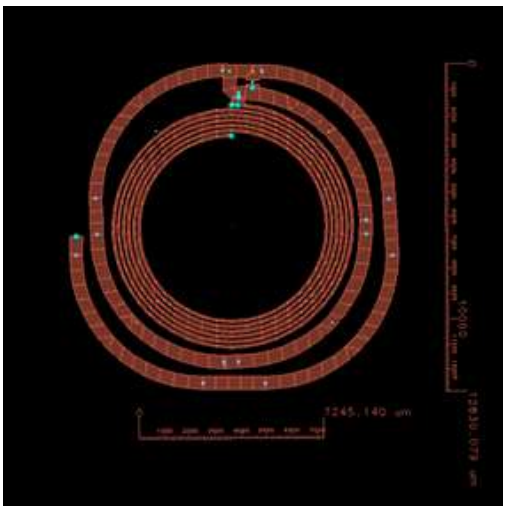

Figure 13: Third antenna design, consisting of two separate loops of non-uniform trace width.

This dual loop design uses an inside coil, even though they are not connected, couples into the actual antenna and has a direct effect on the resonant frequency of the outside loop. The loop antenna has a small coupling loop (roughly 1/5 of the size of the antenna), which is fed the signal instead of the larger loop. The thicker loop is the antenna. The outer diameter is about 1.3cm and the inner diameter is about 7.2mm. Using a thicker trace for the antenna, Benny was able to improve efficiency compared to sticking to a uniform trace width.

After all three antenna were simulated, it was determined that regardless of substrate and size, only the dual loop antennas would be appropriate for achieving the desired functionality. Figures 14, 15, and 16 below present the results from these simulation.

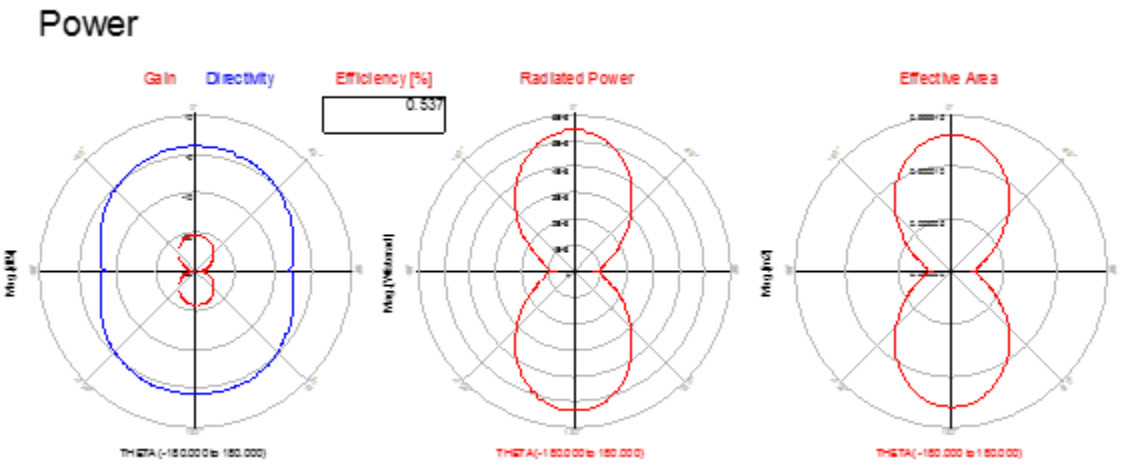

Figure 14: Antenna design 1 efficiency and power results.

Immediately from figure 15 above we see that antenna design 1 will not be a sufficient platform in providing wireless charging. The efficiency, which sits a 0.537%, is too low to sufficiently facilitate power transfer.

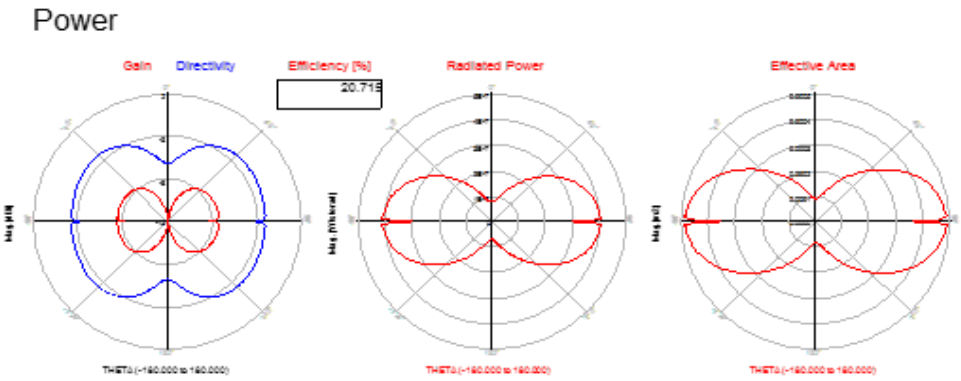

Figure 15: Antenna design 2 efficiency and power results

Antenna design 2, unlike design 1, displays much more promise as a platform for wireless charging. With an efficiency at 20.715%, the design is more than viable for facilitating wireless power transfer.

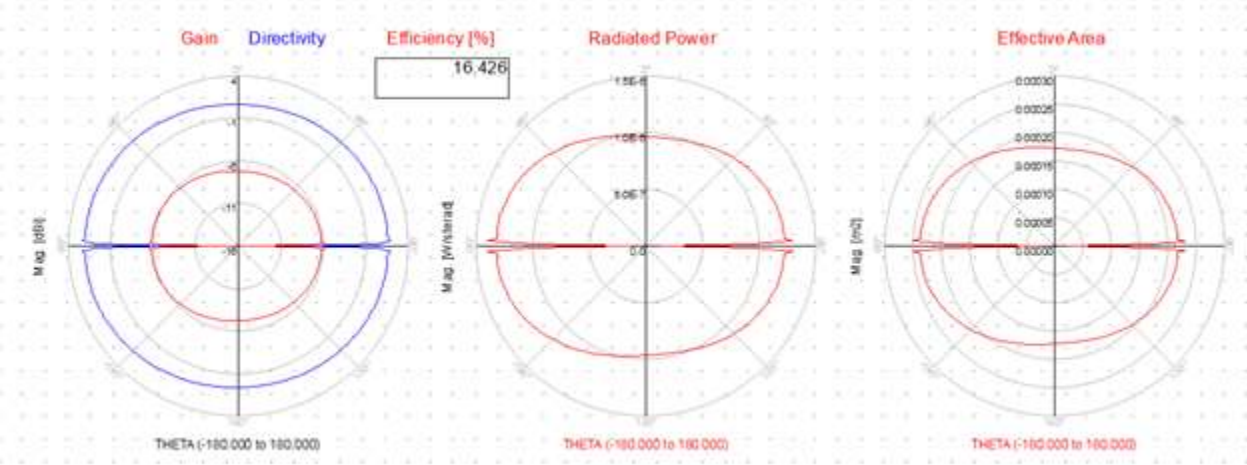

Figure 16: Antenna design 3 efficiency and power results.

Antenna design 3 follows closely in line with design 2, albeit with a lower efficiency. Ideally, all the antenna designs will be able to receive signals regardless of efficiency. To meet our design requirements, however, it was imperative to choose a design that best suited the wireless charging platform. While antenna design 2 represents the highest efficiency, it has a much lower effective area, making it less suitable for wider range of communication distances. Geometrically, antenna design 2 also interferes with our clear vision requirement, just barely clearing the maximal pupil dilation diameter requirement. As such, we decided that antenna design 3 would be the best option to pursue towards the final design.

Battery Design - Charging considerations

During the research phase, different types of portable power supplies (batteries and capacitors) were compared and contrasted. Not only was power, size, and flexibility a concern, but also health hazards from the materials being used. Graphene supercapacitors represent a potential answer to these requirements. Supercapacitors have unique properties that make them an attractive choice as a power source. They are essentially maintenance-free, possess a longer cycle-life, require a very simple charging circuit, experience no memory effect, and are generally much safer [14]. Also, one of the key characteristics of a supercapacitor is that it can be charged and discharged at high rates.

Graphene is a two dimensional crystalline allotrope of carbon where the atoms are densely packed in a sp2-bonded hexagonal pattern [15]. Graphene can be described as the top skin layer of graphite. High quality graphene (pristine graphene) is not only an excellent conductor, but it is also strong, flexible and nearly transparent. The conductivity of a single-layer graphene sheet has been measured up to 649 S/cm [16]. The most important property of

graphene with respect to supercapacitors is the high theoretical specific surface area of 2675 m^2/g which corresponds to a theoretical specific capacitance of 550 F/g [14]. The target capacitance value for the fabricated supercapacitor that was calculated is 32mF.

Unfortunately, graphene supercapacitors are highly experimental. Even after conducting large amounts of research into integrating the technology into our lens, our group was unable to fabricate the component in a reasonable time frame. Thus, we decided to use the current paradigm of thin film lithium ion batteries, which are readily mass produced by manufacturers such as Cymbet. While not as flexible and thin as a graphene supercapacitor, thin film lithium ion batteries are affordable and easy to use, making them a good choice to demonstrate our embedded power platform. One such battery is shown in figure 18 below. Unfortunately, this battery is not appropriate for the final implementation of the contact lens due to biocompatibility issues with lithium.

Figure 17: Thin film lithium ion battery, with penny for scale.

Integrated Circuitry - Protection considerations

The majority of the design selection process in this project stemmed from requirement considerations associated with the battery and the antenna. The integrated circuitry will work on all of the proposed designs, regardless of substrate, size, and charging platform. The circuitry, however, must operate such that it is not damaged by the discharging of the thin film battery and the radiofrequency transmission from the antenna. Therefore, much of the design work on the integrated circuitry revolved around designing protection circuitry ensuring both regulated charging voltage and low battery voltage cut off to preserve battery longevity. The new complete circuit is shown in the figure 18 on the next page, with accompanying charging circuitry:

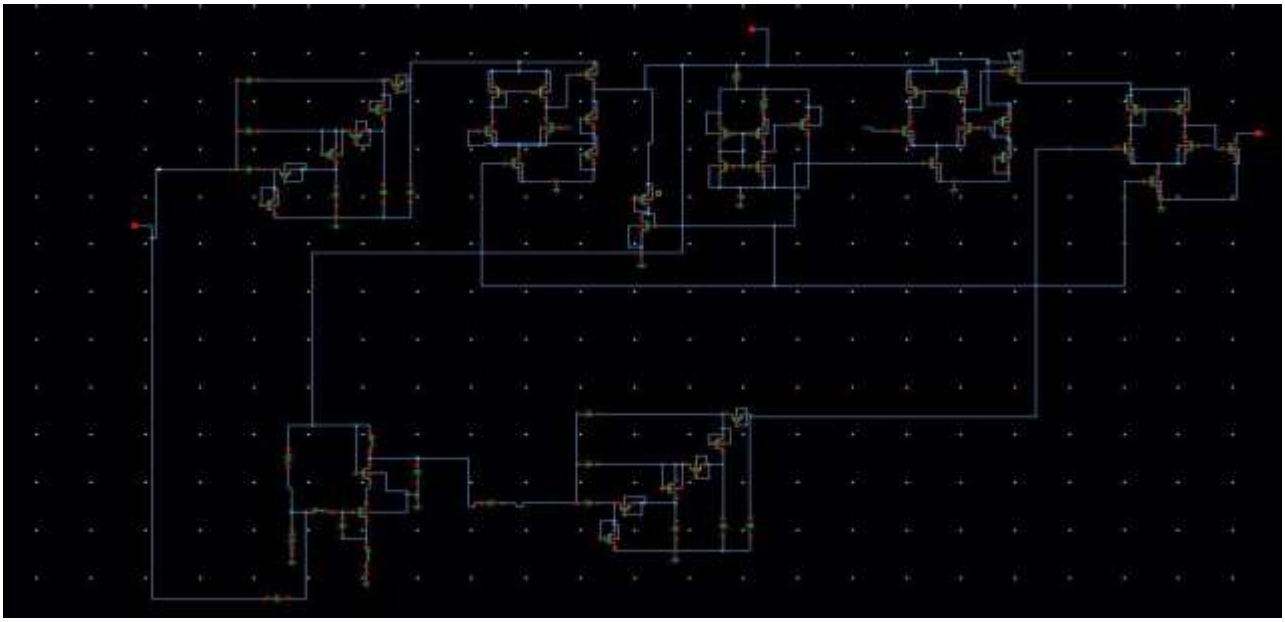

Figure 18: Integrated Circuit schematic, including input and output terminals.

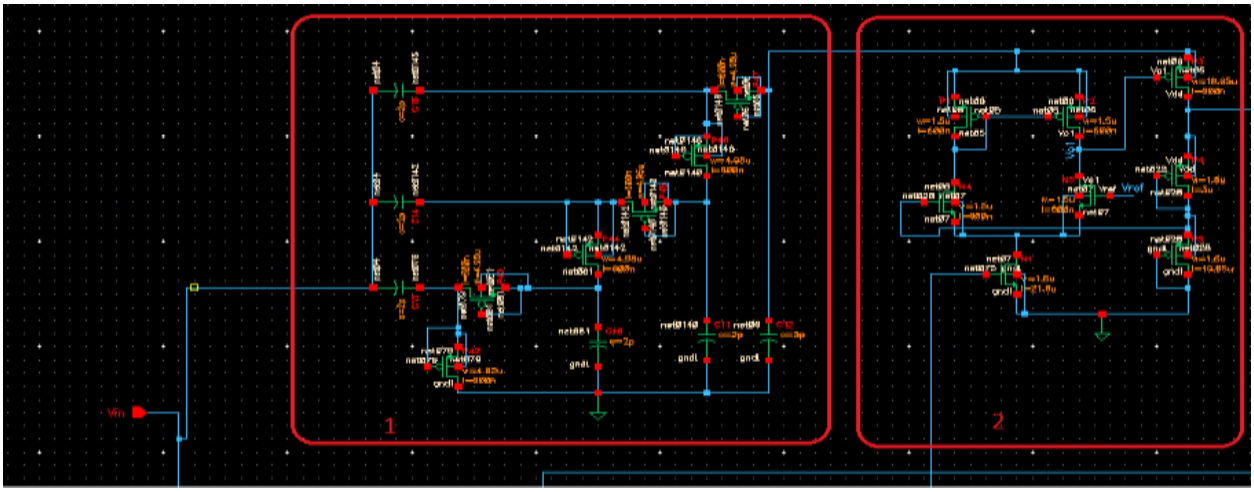

Figure 19: Enhanced image of charging circuitry.

The two red boxes above indicate the new protection circuitry developed this quarter. In box one, a three stage charge pump rectifies an input sinusoidal wave to ensure it matches specific requirements listed in the appendix. In box two, a voltage regulator clamps the charging input voltage to 4.1 volts to ensure that the batter receives optimal voltage and is not damaged during charging.

VI Final Design

Our final design consisted of a circuit platform embedded in PDMS. The base of the lens consisted of a printed antenna upon a PET substrate. The printed and insulated electro chromic ink lays on the same layer as the PET. There are additional printed insulation layers on top of the antenna upon which the battery and IC are bonded using a thermo-epoxy. The battery, IC, and electro chromic are connected via wire-bonding, which can be seen in Figure 2 on the next page. The entire system is embedded in PDMS.

Our modular focus for the analysis and testing of device components resulted in a well-defined set of geometries and component characteristics that integrated to form our final device. IC simulations using Cadence Virtuoso showed a total current draw of 5.41uA. Inductive charging required 4.5Vp at the input of the chip. The display will activate when the IC sees 1 dBm from the wireless sensor. Based upon the desired material characteristics and size constraints of the Antenna and IC, the geometry of the lens was designed to match the curvature of the eye as closely as possible. The edge-to-edge diameter of the lens was 1.5 cm, with a thickness of 950 ums. This allowed for a 50 um layer of PDMS on the top and bottom of the lens with 200um of edge coverage.

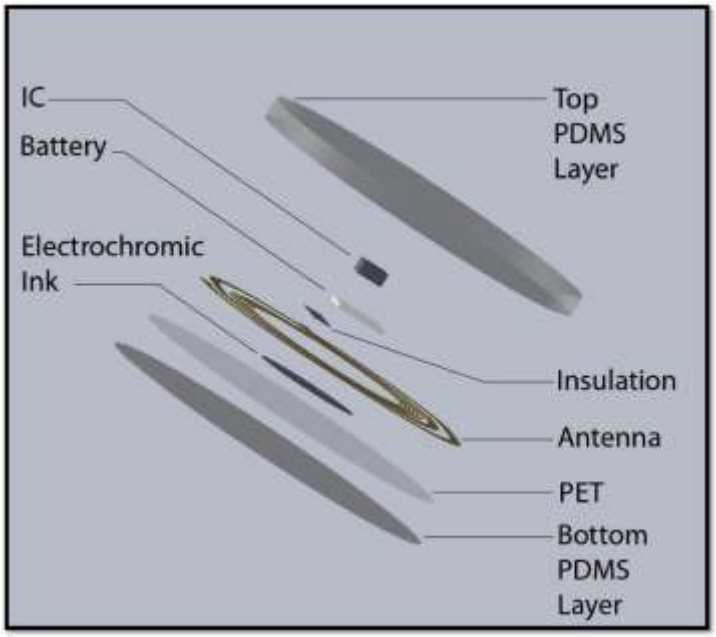

Figure 1: Exploded view of lens highlighting individual layers and components. Wiring has been removed for clarity.

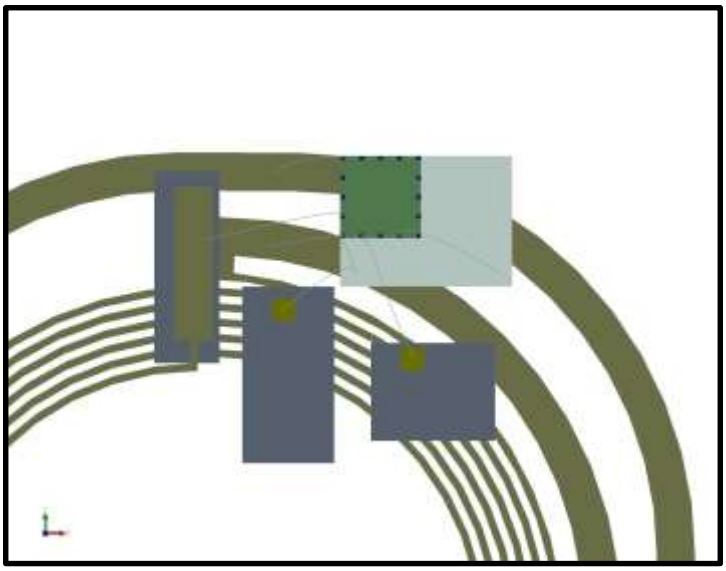

Figure 2: The wiring schematic above shows interconnections between device components.

Analysis Results

Preliminary analysis of various aspects of the initial three designs indicated the chosen final design was not only the most feasible option, but also the most robust. Bioheat analysis of PET and PDMS indicated that both polymers would be suitable for the construction of a lens exposed to a constant 10 mW power dissipation. By encapsulating a PET frame in PDMS, however, an extra layer of thermal insulation is created, and it is possible to further isolate the eye from the power dissipated by the lens. Theoretically, this will decrease the temperature of the cornea when the device is active, and provide for a more comfortable experience.

From a functionality perspective, the antenna design played a role in choosing this design. While 2 cm would allow us to achieve a higher efficiency, a 1.5 cm is a more contemporary size for contact lenses. Many individuals do not wear scleral lenses as they are larger and more uncomfortable. From a manufacturing perspective, while 1.5 cm lenses are smaller, the difference is negligible in terms of modern machining tolerances and would be supported as well as a 2cm design.

Cost Breakdown

The costs below do not include materials supplied by Cal Poly such as screens, PET, PDMS, or access to facilities. This project was focused heavily on R&D.

- $500 CNC tech hours + materials
- $1744.95 R&D graphene supercapacitor
- $323.94 Electrical components and thin film battery

Total Expenses: $2568.89

Safety Considerations

With any biomedical device, biocompatibility is a top priority. Ensuring that the body does not harm the device and the device does not cause harm is the foundation of medical engineering, and in our case this applies even more readily since the contact lens is interfaced with a highly sensitive organ. Materials selection should be noted here as a point of special consideration. PET was found to be, according to a study conducted in 2010, an endocrine disruptor when exposed to a biological system [17]. This is a definite problem when applied to all three designs. A design that incorporates a barrier between the PET and the surface of the eye would be the most desirable to counteract this finding.

While literature reviews of PDMS have indicated it is a biocompatible material with minimal side effects we do not advise usage of lens for extended periods of time. Both in vitro and in vivo testing must be done before the lens can be safely used. These tests are also critical, because they account for parameters that are difficult to measure, such as the leaching behavior of the PET, electrochromic ink, lithium battery, or substances from the bare die IC using simulation. At this point, safety concerns have been addressed as much as possible to ensure a device that is both safe and effective.

Maintenance and Repair

Since this device is acting as a contact lens, user maintenance of the device is critical. Traditional contact lenses are stored in a saline solution overnight to prevent build-up of proteins over time. Additionally, while PDMS is oxygen permeable, the eye still does not receive as much oxygen as if it were exposed to the atmosphere. Therefore, the user will likely be instructed to remove the lenses after 8 hours or less similar to traditional lenses. While the user may be able to wear the device for up to 8 hours, the device will only be functional for 1 hour, after which it will need to be recharged. Recharging time is estimated to be less than 1 hour, and could increase in the future as battery capacities grow. Lastly, the electronics in the device are completely encapsulated, rendering any attempts at repair unlikely. The device will likely act as a monthly or yearly lens to reduce cost of replacement.

Differences from Planned Design

Our final prototype departed from our final design due to a delay in the IC fabrication process. Without the IC, it was impossible to assemble a complete circuit. As a result, focus was placed on developing the manufacturing process used to create the lens. The final lens incorporated the PET antenna, battery, and PDMS encapsulation to come as close as possible to the final design within our resources.

VII Project Realization

Manufacturing Process

The lens manufacturing process was designed to be simple and robust. The process overview involves four major steps: printing the lens, curving the lens, attaching the components, and embedding the circuit in PDMS. To carry out this process, manufacturing techniques from across disciplines were used. Screen-printing machines in the GrC department were used to fabricate the antennas. The molds were designed using SolidWorks in the BMED computer lab and manufactured in the Bonderson Machine shop. The PDMS was mixed and degassed using the Micro fabrication lab facilities.

Outline of Manufacturing Process

1. Screen Print Antenna
2. Attach PET Substrate to Male Mold 1
3. Place Mold in oven at 180 degrees Celsius for 10 minutes
4. Attach components using thermo-epoxy
5. Use Mold 2 to build top layer of PDMS
6. Use Mold 3 to build bottom layer of PDMS

Step 1:

The first step in screen printing is to develop a mask of the design you want. The mask, seen below in figure 1, is designed using Adobe Illustrator and printed using the Cyrel Digital Imager, seen below in figure 2.

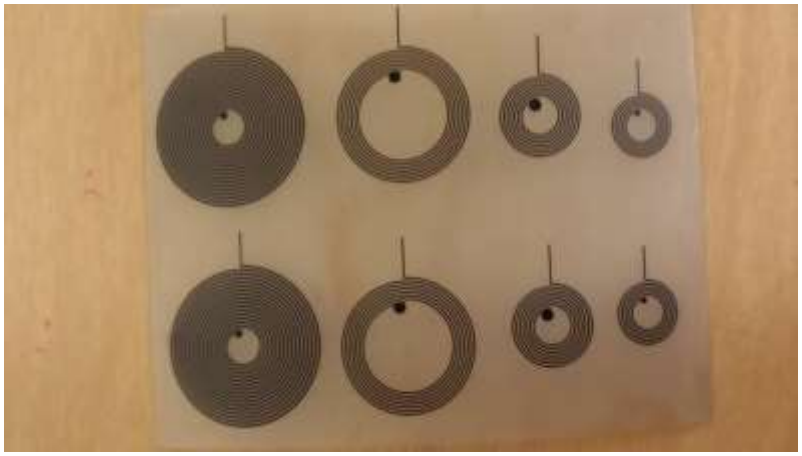

Figure 1: Mask for antenna fabrication.

Figure 2: Cryel Digital imaging machine printing antenna mask.

The next step requires applying an emulsion layer to a 420 lines per linear inch mesh. This is very fine screen size that allows features of up to 10 um to be printed. The emulsion was then cured using UV light. The mask was placed in between the screen and the UV. The areas of the mask that block the UV light prevent the emulsion from curing. This allows it to be washed away, as seen in figure 3 below. This process must be done in a dark room to prevent light from curing emulsion and preventing its removal. If emulsion cures it will remain on the screen and create holes in the final printed antenna design.

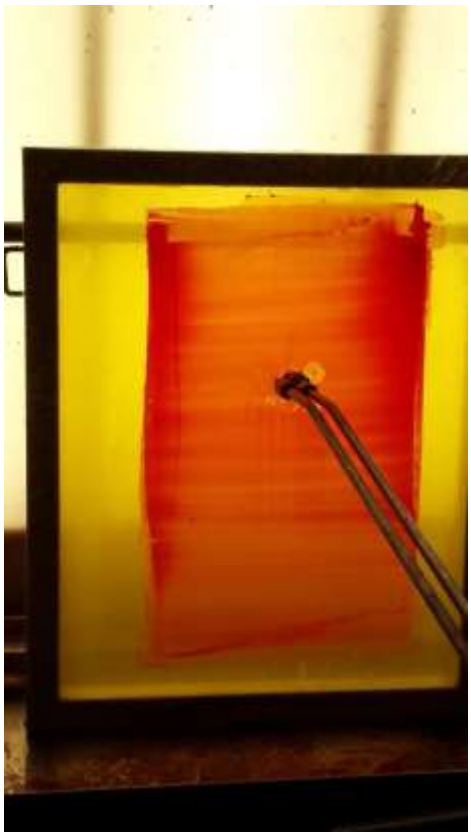

Figure 3: Removal of emulsion to create screen features.

In the final step of this process, the PET is placed on the machine, on top of which the screen is placed. The ink is then applied and the automatic applicator is engaged. It is critical to apply the silver ink quickly and engage the applicator, otherwise the ink will dry and ruin the features of the antenna. This process can be seen below in figure 4. The final product can be seen in figure 5 on the next page.

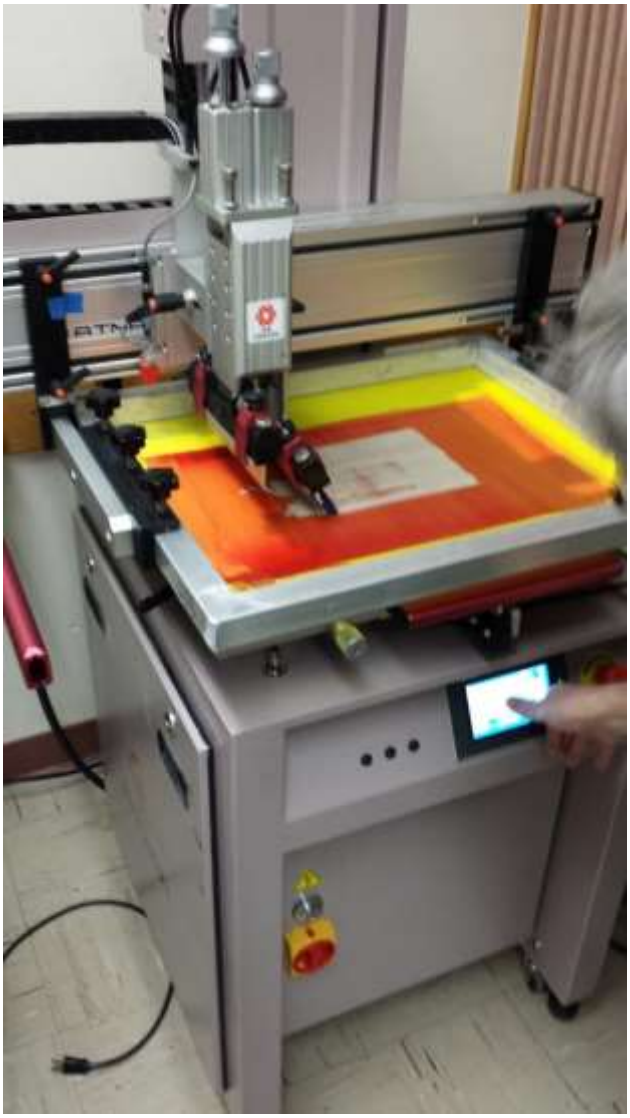

Figure 4: Application of the silver ink using the ATMAS machine.

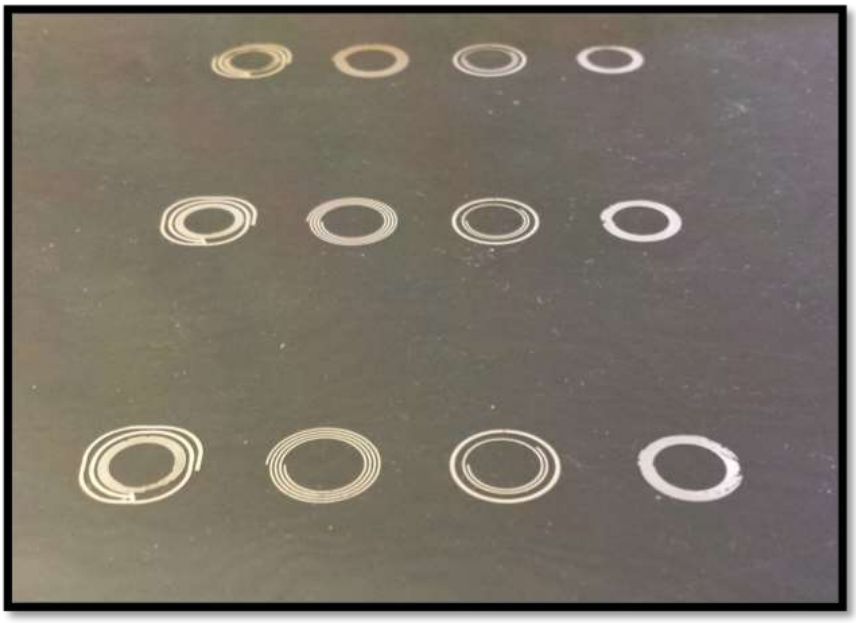

Figure 5: Printed antennas on PET substrate.

Step 2 and 3:

The PET with the printed antenna is a planar object. To properly orient the antenna on the mold, the antenna is manually centered on the male component of the mold and taped into place on the side. The Female Mold 1 is then placed on top of the Male Mold 1 and placed in the oven at 180 degrees Celsius. After 10 minutes, the mold is removed from the oven. The oven and mold are both hot, so it is important to insulate all body parts from the heat. The mold is then left to cool for 15 minutes down to room temperature. The mold is then separated and a representative image of the result can be seen in figure 6 below.

Figure 6: Molded PET antenna.

Step 4:

The components are then attached to the device using a thermo-epoxy. This step was not completed during the course of this project, as not all components were available. This will be completed in the near-future.

Step 5 and 6:

The encapsulation of the lens in PDMS occurs in two stages with two separate molds. For the first mold, PDMS is poured into the bottom of Female Mold 2. The PET lens is then attached to the center of the male component, and placed component side down into the PDMS. A common issue with PDMS is the formation of bubbles during the pouring process. To overcome this, the mold is then placed in the degassing chamber to remove all bubbles that have formed. The mold is then place into the oven at 70 degrees Celsius for 4 hours to cure. For the second stage of the process, the lens is placed PDMS side down into the third mold, and the PDMS is poured onto the PET side making a small pool and can be seen below in figure 7. The male component is then inserted, and the cavity formed creates a 50um layer of PDMS on top. The lens is then cured again for 4 hours at 70 degrees Celsius.

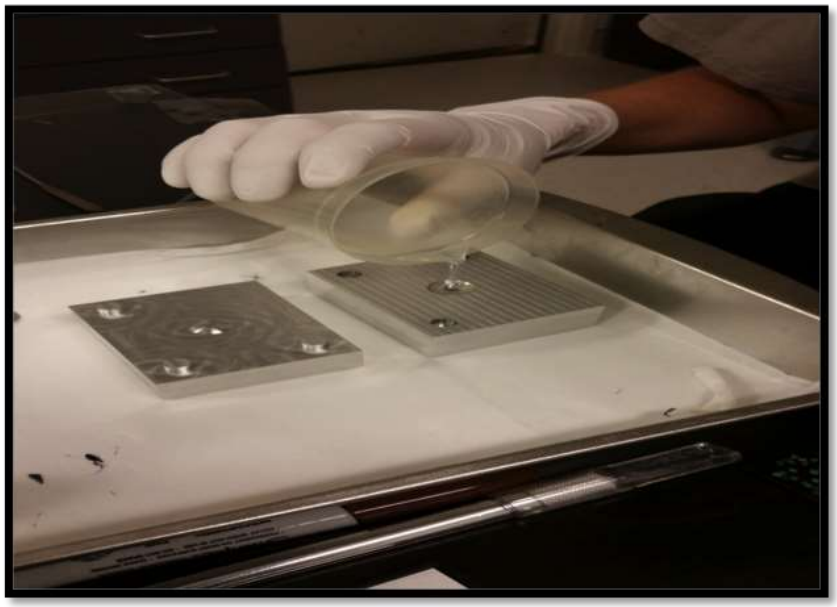

Figure 7: Pouring of PDMS to form external lens layer.

Difficulties and Recommendations for Future Designs:

Curving of the PET lens proved to be a much easier process than expected, however it still had its challenged. Wrinkle formation was a problem, as many times the edges of the antenna would have a fold or two. However, the center of the lens usually stayed free from wrinkles. In the future to prevent this, I would use a much large male sphere over which to pull the PET. This would help to ensure that the antenna at the center of the lens was free from wrinkles and damage.

Forming the PDMS encapsulation layer provided multiple challenges including separation of the mold following degassing and rouge edges. Following curing of the mold, it was impossible to separate the male and female components by hand. Eventually, a razor blade and a hammer were used to pry it apart. It was found that excess PDMS had escaped from the center of the mold and dried in between the male and female mold faces. It was likely the bond between the PDMS and the mold is what made it difficult to separate them. Apparently this is not an uncommon occurrence in inject molding, and a simple solution is to machine a bevel in the side similar to ones on a laptop to make it easier to pry open. To remove the rough edges of the PDMS, manufacturing a separator similar to a cookie cutter would eliminate many of the problems associated with manual removal via exact knife, such as rough edges and damage to the mold itself.

VIII Design Verification and Results

To verify the final design, testing on both individual components and the final manufactured lens was conducted. Each test was designed with the sole purpose of evaluating the specific components ability to meet the design requirements put forth at the beginning of the project. Table I below summarizes the testable design requirements.

Table I: Design requirements

	Clear Vision
1	Substrate material refractive index between 1 and 1.5
2	All circuitry outside of a 9 millimeters +/- 1 millimeter
3	Substrate water contact angle of ~60 +/-5 degrees
	Comfortable
4	Sufficiently biocompatible substrate.
5	Thickness of no more then 400 micrometers
6	Sufficiently breathable substrate material
7	Temperature of the cornea does not vary by more than 1.5 degrees Celsius.
	Isolated Functionality
8	1 Minute operating time, 1 +/- 0.5 micro ampere-hour
9	2.4 GHz IEEE compliant RF communication
10	10 milliwatt +/- 5 milliwatt maximum power dissipation

Clear Vision

The focus of testing performed to assess the clear vision requirement was to ensure that the product caused the least interference with the users vision at all times. As such, elements such as refractive index, circuit geometry, and contact angle were analyzed.

Refractive Index Testing

In refractive index testing, a simple fixture was created using equipment found in the Biomedical Engineering Lab of Engineering IV. The following materials were used: 650 nm, 10 mW laser pointer, solder assist clamps, tape measurer, a level, protractor, a white board, and whiteboard markers. Figure 1 on the next page shows some of the materials used in proving the fixture.

Figure 1: Materials used in designing refractive index test fixture.

The fixture involved attaching the laser pointer to a protractor, placing it on a level surface, and fixing the test subject at a point at least 2 feet from the laser pointer. The laser would then be directed using the protractor at the subject material, in this case the contact lens, at varying angles. A white board placed behind the lens would be used to mark the location of refraction through the lens, and after measuring the x and y distances from the lens, the angle of refraction would be computed using trigonometry. Using Snell's law, the refractive index of the lens would then be determined. After 15 different attempts, data collected was discarded due to a standard error that exceeded a tolerance of more than 3 standard deviations away from the average.

This test ended inconclusively for a number of reasons. The first most jarring reason was the difficulty in controlling the absorption of the laser as it entered the lens. Since the lens is a compound material composed of two PDMS layers around a PET skeleton, there is a high chance that some of the light will be absorbed and dispersed as it passes through the lens. This effect was so noticeable, in fact, that the prototype incurred thermal damage when examined immediately following the first test. To account for this effect, future tests should include calculations to determine if the effect of absorption will damage the lens, and therefore make determining refractive index impossible. Another challenge associated with ascertaining the refractive index is the nature of the test itself. At the time when the tests were performed, it was assumed that the light exiting the lens would be refracted. This is, however, not correct, as light exiting the lens will retain the angle at which it entered, since it is reentering the medium in which it originated. This is in accordance with Snell's law of refraction. As such, it may be more appropriate to purchase a refractive index tester, such as one manufactured by Presidium Electronic, to determine the refractive index accurately.

Circuitry and Antenna Printing Verification

This phase of verification involved determining whether or not the screen printing method of manufacturing the antenna produced consistent inner diameter free of obstruction. Materials used in this test include calipers accurate to 3/1000th of an inch, 20 screen printed antennas, and the prototype lens. Figure 2 below shows an example of this test using a ruler.

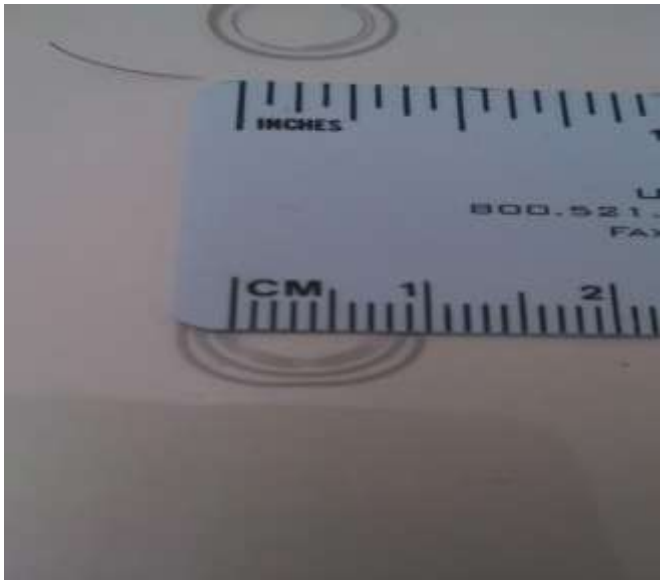

Figure 2: Example of antenna printing verification.

The result of measuring many antennas including the prototype lens revealed that the printing process is a remarkably accurate manufacturing method. Nearly all antennas were printed with an inner diameter of 8 mm, within the tolerance threshold for the specification. Out of twenty printed antennas, only 2 had defects associated with the arduous process manually screen printing the antennas. These defects caused a slight smearing of ink into the center of the lens. Since the sample size is very small, no statistically powerful conclusion can be made regarding the accuracy of the printing process, but for our design, an error rate of 10% that creates visibly distinguishable defects is very good.

Since all other circuit components will be laid on top of the antenna and outside the inner circle of the contact lens, this test remains a good measure of determining how strongly the circuitry will interfere with vision, if at all. A more in depth test could be performed with a contemporary contact lens in order to verify the minimum clearance diameter of 9 mm. Using a non-toxic marker, a circle of 9 mm would be drawn onto the surface of a contact lens prior to application. Then, the subject would wear the lens and enter a dark room to ensure maximum pupil dilation. If the subject is able to distinguish the colored circle in their vision, then our chosen 9 mm threshold radius is too small.

The three printed antenna designs were tested for performance and far-field characterization using the microwave lab equipment and a test antenna.

Equipment:

17cm reference antenna/transmitter

Anritsu MS4622B Network Analyzer

CXA Signal Analyzer

Synthesized Sweep Generator

Figure 3. Antennas under testing. AUT1, AUT2, AUT3 from left to right.

List of test parameters:

1. Gain
2. Impedance and Bandwidth
3. Polarization and Beam width
4. Radiation pattern (magnitude)
5. Efficiency

1. Gain Test

The transmitter has an unknown gain, which can be determined by testing the received power of each AUT and reference antenna. This test will also determine the gains for all 3 AUTs. Using a set of four conservation of power equations and four unknowns, we can calculate the gains of each antenna.

$P_{R_{ref-1}} = P_{TX} + G_{ref} + G_1 - PF$ $\quad$ $P_{R_{ref-2}} = P_{TX} + G_{ref} + G_2 - PF$

$P_{R_{ref-3}} = P_{TX} + G_{ref} + G_3 - PF$ $\quad$ $P_{R_{1-2}} = P_{TX} + G_1 + G_2 - PF$

In order to accurately test the antennas under far-field condition, we must first determine the far-field range, which is $R \geq {}^{2D^2}/_{\lambda}$, where D is the length of our source reference antenna and λ is our operating wavelength, 12.5cm.

$R \geq {}^{2(17cm)^2}/_{12.5cm}$

$R \geq 46.24cm$

Figure 4. Antenna gain test setup for 2.4GHz far-field range of 50cm

We will use a distance of 50cm for the entirety of our tests. At 50cm, the path loss at 2.4 GHz is calculated with free space approximation.

$$FP(dB) = 10log\left(\frac{4\pi d}{\lambda}\right)^2$$

FP = 34dB

Our power transmission test setup includes the reference antenna mounted 50cm away from the test antennas and transmitting 1dB from the frequency generator. The test antennas are mounted on the SMA adapter for easy swapping. The measured received power from the reference antenna to antenna 1 to be -44.77dBm, as seen in Figure 5. The measured received power from the reference antenna to AUT 2 to be -42.19dBm, as seen in Figure 6. The measured received power from the reference antenna to AUT 3 to be -44.57dBm, as seen in Figure 7. The measured received power from AUT 2 to AUT 1 to be -57.55dBm, as seen in Figure 8. Before any calculations, we can already tell that our reference antenna has a higher gain than AUT 2 when comparing the received power at AUT 1.

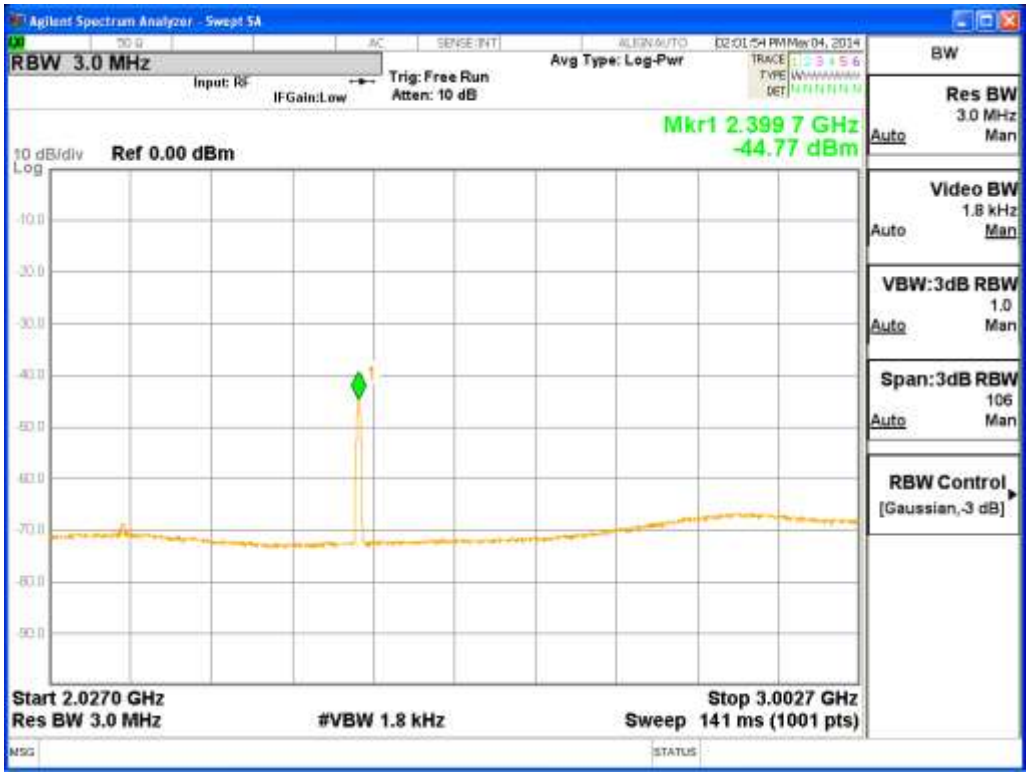

Figure 5. Reference antenna transmitting 1dB to AUT 1 at 50cm

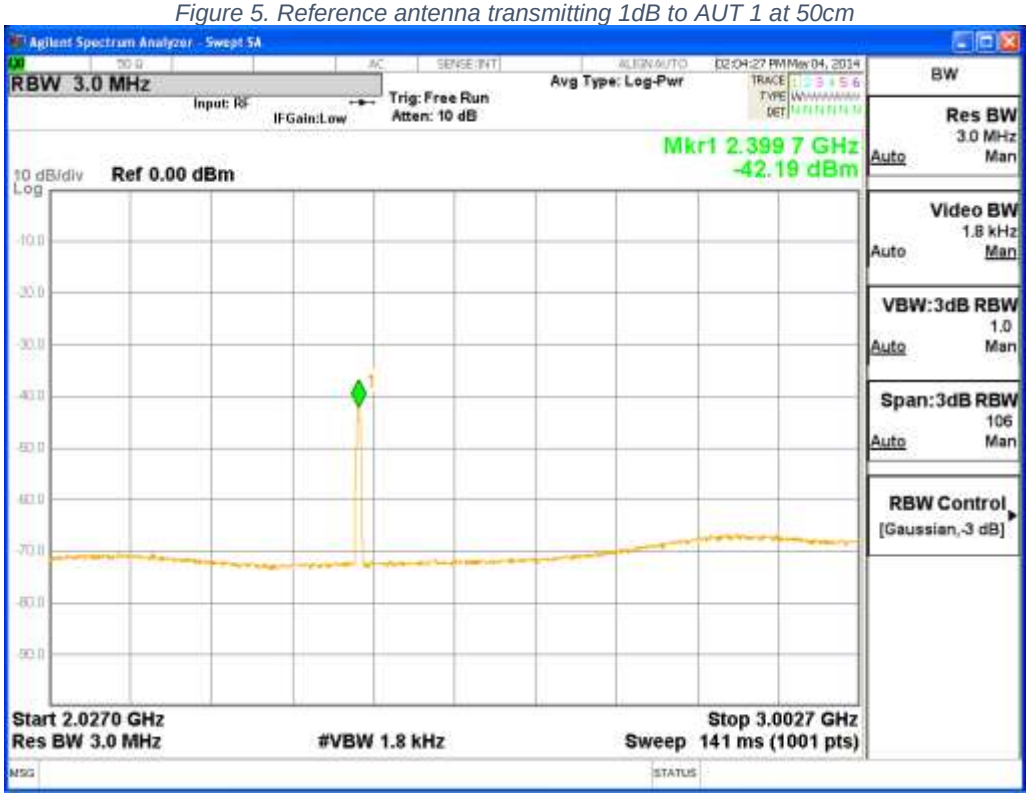

Figure 6. Reference antenna transmitting 1dB to AUT 2 at 50cm

Figure 7. Reference antenna transmitting 1dB to AUT 3 at 50cm

Figure 8. Antenna 2 transmitting 1dB to AUT 1 at 50cm

Solving the conservation of power equations with the received power data gives us the gains for each antenna.

$-44.77 = 1 + G_{ref} + G_1 - 34$ $\quad -42.19 = 1 + G_{ref} + G_2 - 34$

$-44.57 = 1 + G_{ref} + G_3 - 34$ $\quad -57.55 = 1 + G_1 + G_2 - 34$

$G_{ref} = 1.7950\ dBi$, $G_1 = -13.565\ dBi$, $G_2 = -10.985\ dBi$, $G_3 = -13.365\ dBi$

2. Impedance and Bandwidth Test

Using the Anritsu MS4622B Network Analyzer, we measure the antennas' impedance and bandwidth from their reflection coefficient (Γ), S11 parameter. The measured impedance and reflection coefficient for UAT 1 obtained from figures 9 and 10. The measured impedance and reflection coefficient for UAT 2 obtained from figures 11 and 12. The measured impedance and reflection coefficient for UAT 3 obtained from figures 13 and 14. These measured values and calculated power-ratio, VSWR, and percent reflected power are compiled in Table 2 below.

Parameter	AUT1	AUT2	AUT3
S11 (Γ) [dB]	-5.722	-2.346	-3.476
Power-ratio	0.2678	0.5826	0.4492
VSWR [dB]	1.73	3.79	2.63
Reflected Power [%]	7.2	33.9	20.2
Impedance	19.744-j22.993	13.003-j49.497	194.772+j281.877

Table 2. Antenna parameters calculated from reflection coefficient

Sample calculations:

$Power - ratio = 10^{\frac{\Gamma}{10}}$ For AUT1, $10^{\frac{-5.722}{10}} = 0.2678$

$VSWR = \frac{1+power-ratio}{1-power-ratio}$ For AUT1, $VSWR = \frac{1+0.2678}{1-0.2678} = 1.73$

$Reflected\ Power(\%) = 100 * |\Gamma|^2$ For AUT1, Refl. Power = 100%*0.2678^2 = 7.2%

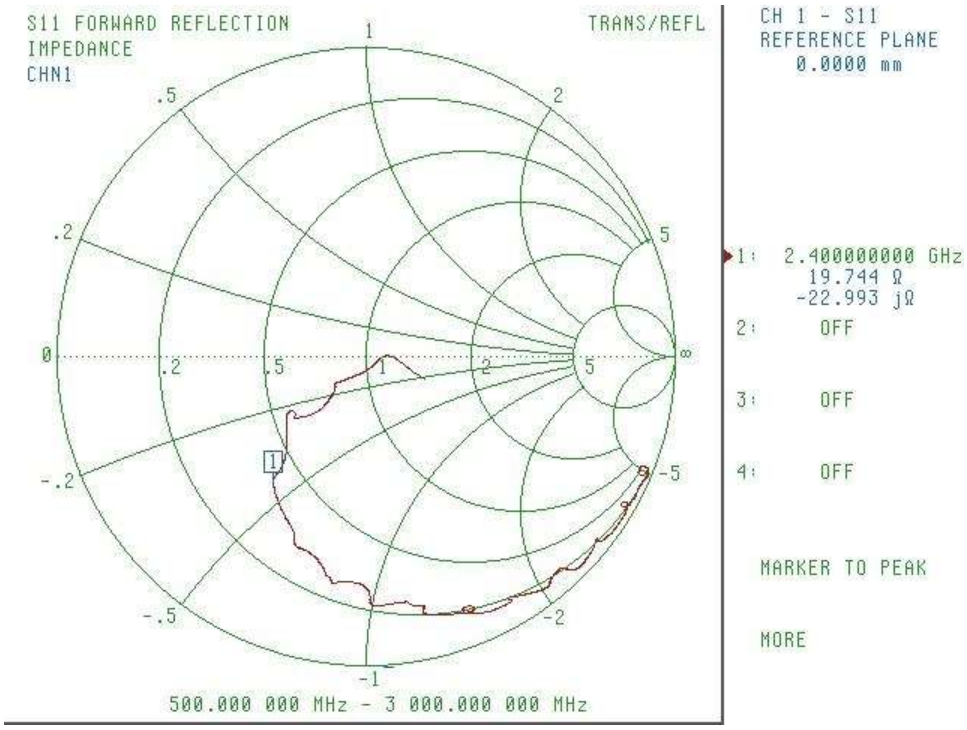

Figure 9. AUT 1 S11 smith chart

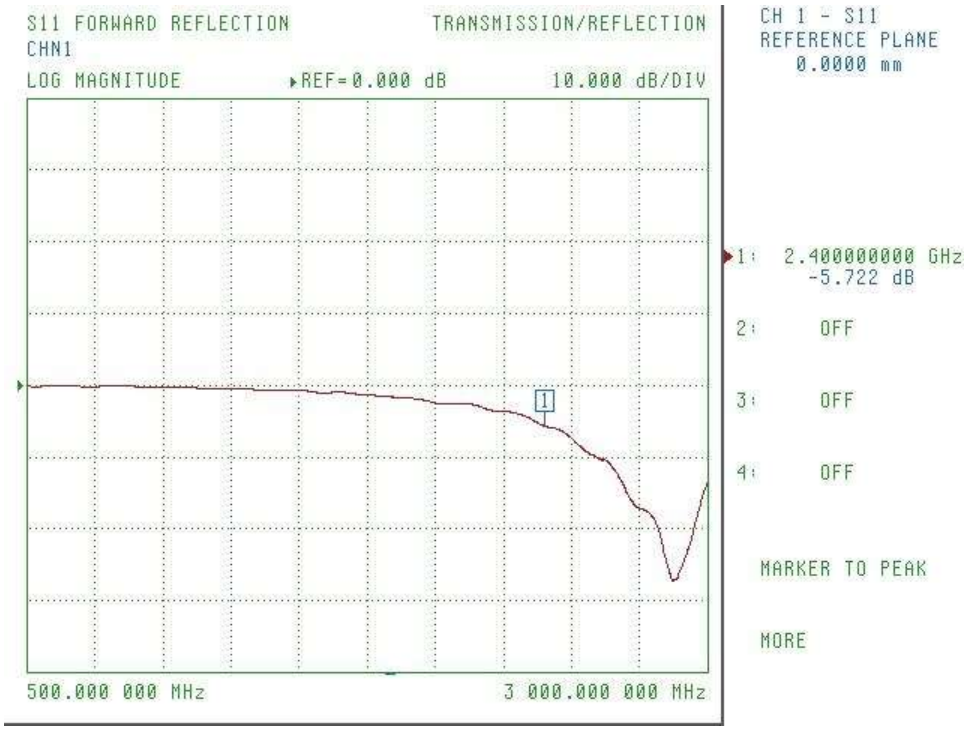

Figure 10. AUT 1 S11 magnitude

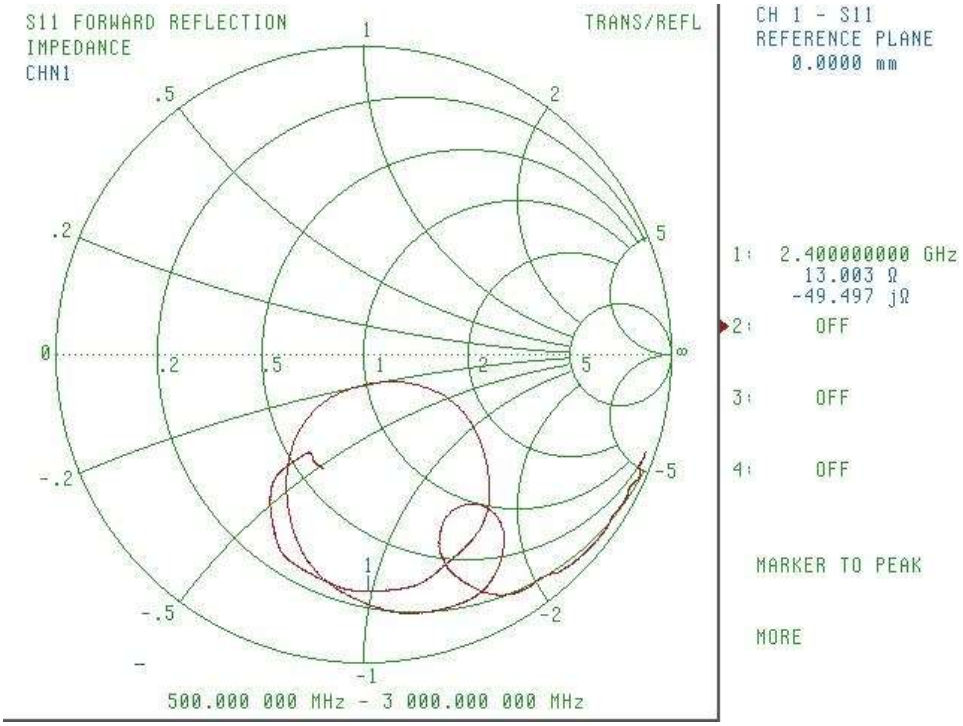

Figure 11. AUT 2 S11 smith chart

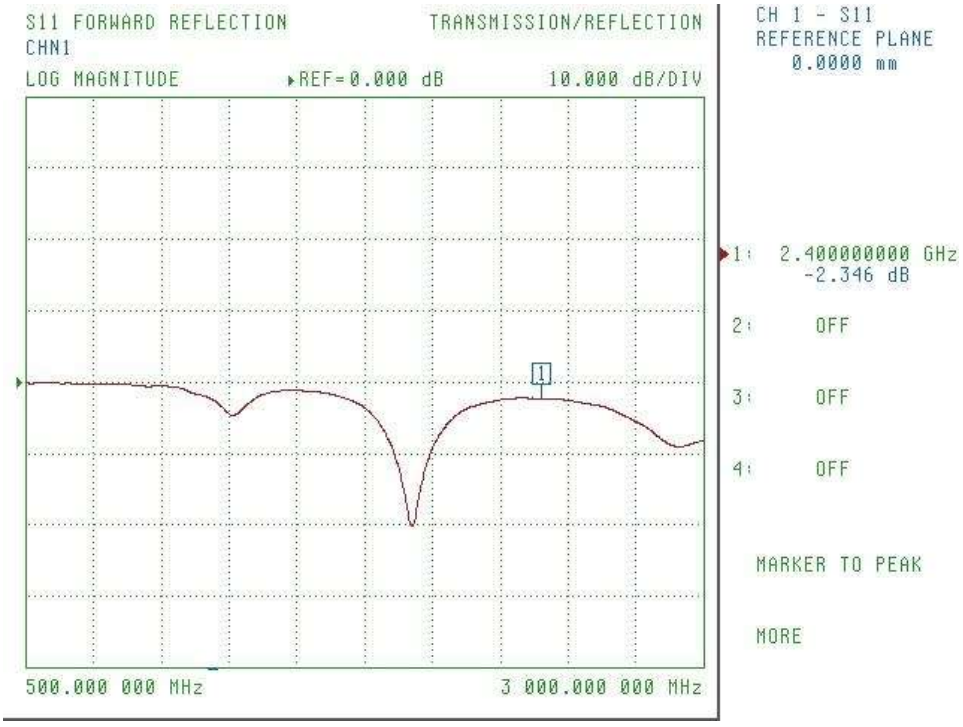

Figure 12. AUT 2 S11 magnitude

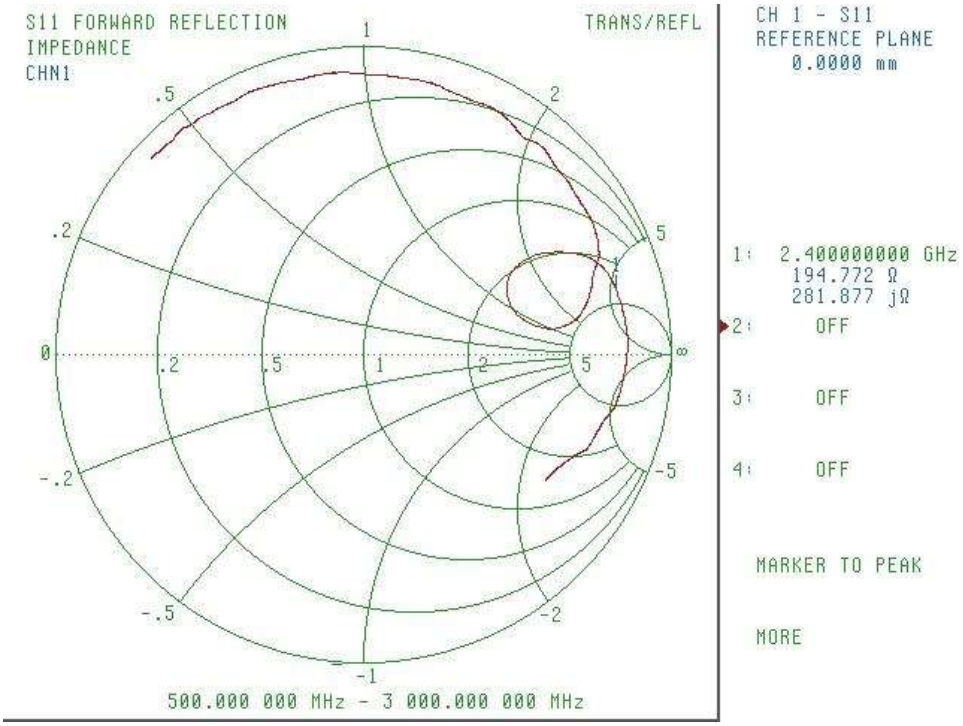

Figure 13. AUT 3 S11 smith chart

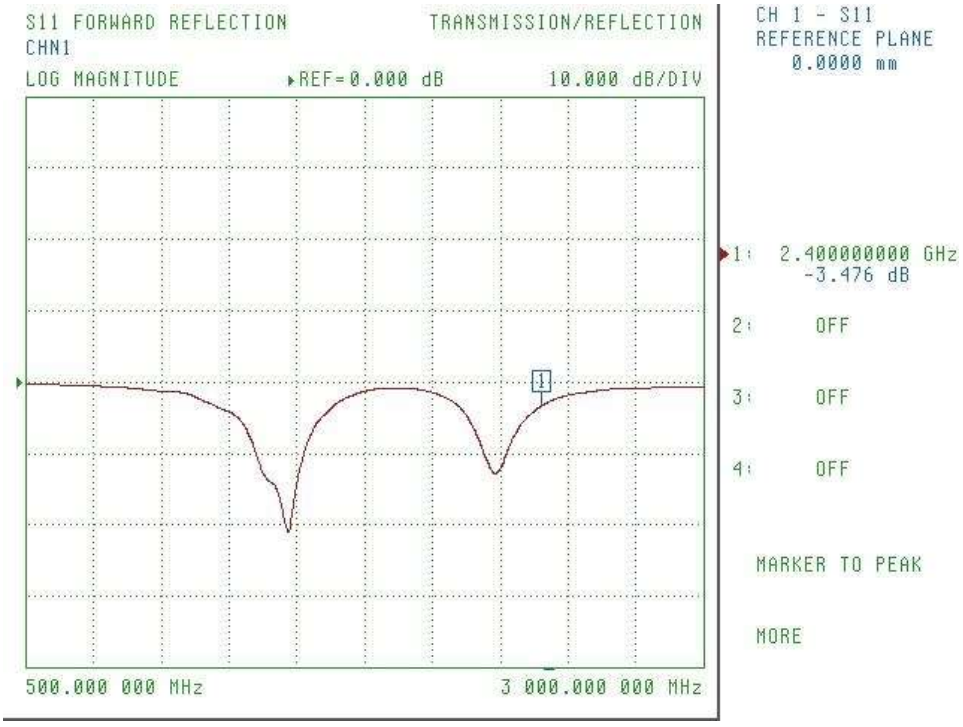

Figure 14. AUT 3 S11 magnitude

3. Polarization and Beam Width

We tested polarization of the AUTs by transmitting a 1dB Sine wave at 50cm with the reference antenna and measuring the received power as the AUT is rotated along the x-axis. Received power remained constant at every angle. From this we can concluded that the AUT and the reference antenna are circularly polarized, which contradicts our theory that most dipole antennas are directional and our printed designs are basically soiled dipoles. If either the reference antenna or AUT were directional, then we would not be able to receive any signals. Thus, beam width measurements are not applicable to circularly polarized antennas.

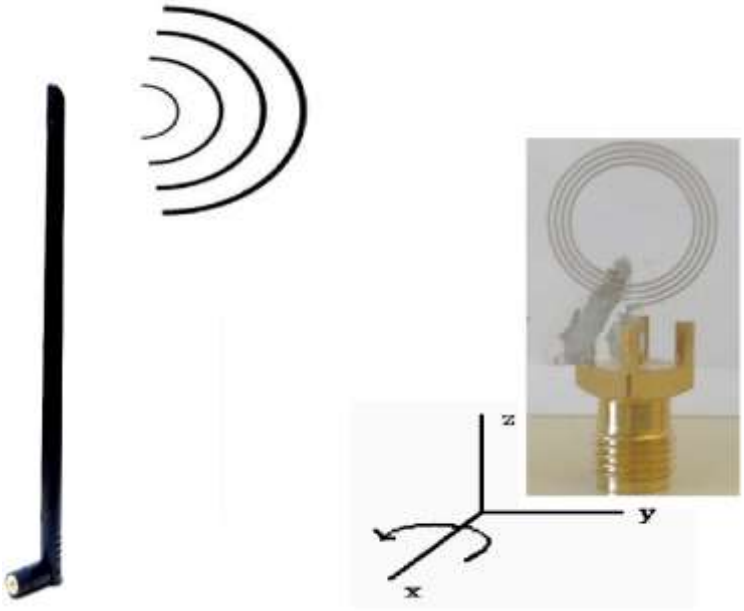

Figure 15. The AUT is rotated around the horizontal axis for polarization measurement

4. Radiation Pattern (magnitude)

To characterize radiation patterns for the AUTs, we transmit 1 dBm signal from the AUT to the reference antenna at 65cm. We measure the received signal and then rotate the AUT about the reference antenna, taking measurements every 20 degrees. The setup required both antennas to be connected to the frequency generator or VNA while orbiting the AUT. The setup was improved three times to find a consistent and efficient method of orbiting the antennas.

Figure 16. The first attempt at measuring radiation pattern required one person to manually holding the mount and ruler and 1 person to record the data. The mount was very heavy. This did not work.

Figure 17. The second setup used a stool to hold the mount instead of a person, but this ran into trouble when the table impedes the testing of the other 180 degrees.

Figure 18. The last setup uses a swivel stool to rotate the reference antenna, which is attached to a meter stick, around the AUT.

Angle [degree]	Ref Rx Power from AUT 1 [dBm]
0	-53.88
20	-38.3
40	-41.67
60	-38.51
80	-41.55
100	-43.77
120	-53.4
140	-52.72
160	-48.93
180	-43.03
200	-46.76
220	-43.88
240	-42.86
260	-40.99
280	-42.14
300	-38.02
320	-39.98
340	-35.54
360	-53.88

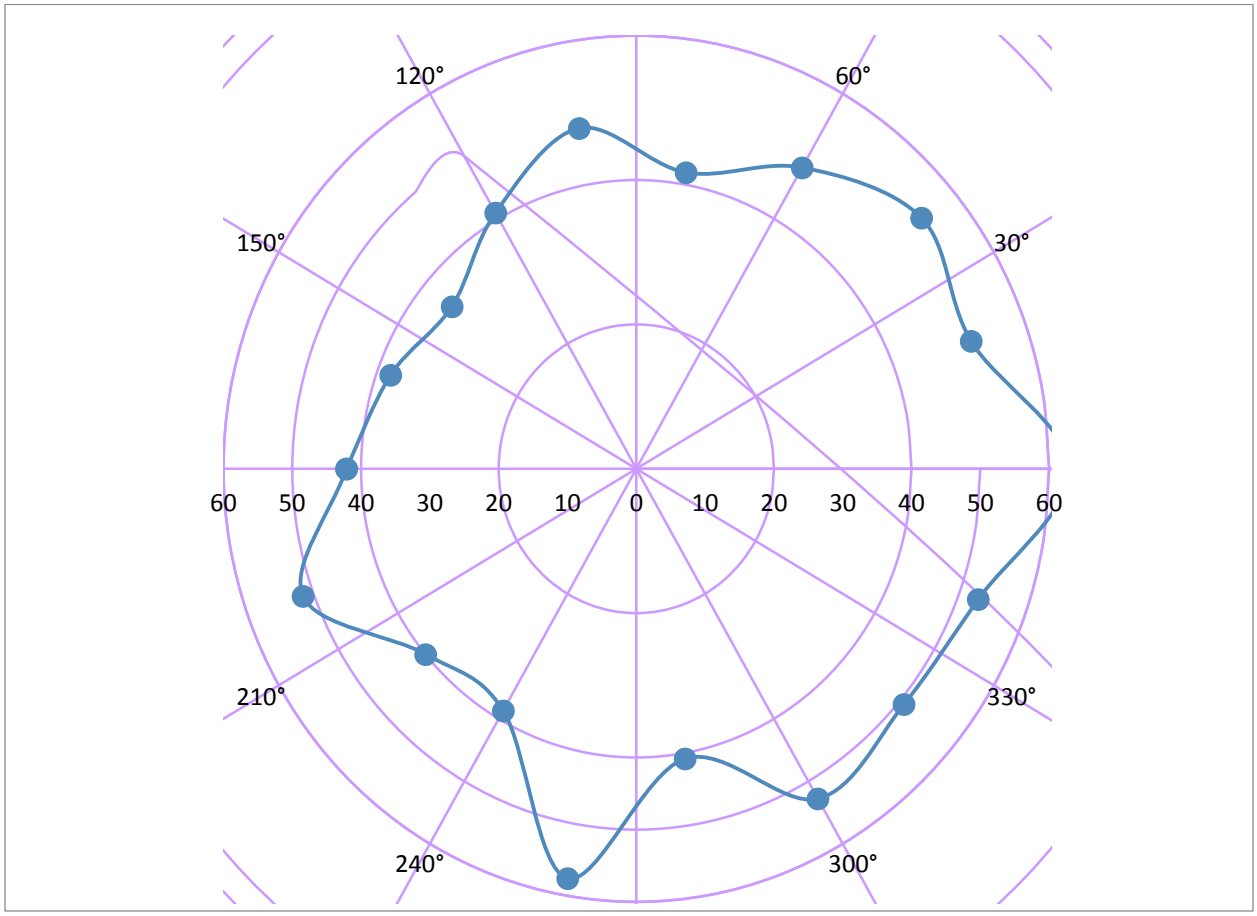

Figure 19. AUT1 Radiation pattern and measured received power

Angle [degree]	Ref Rx Power from AUT 2 [dBm]
0	-55.52
20	-51.75
40	-68.91
60	-53.72
80	-50.1
100	-55.35
120	-54.6
140	-54.96
160	-52.41
180	-63.36
200	-57.11
220	-62.48
240	-68.93
260	-59.54
280	-62.94
300	-59.55
320	-69.53
340	-62.74
360	-55.52

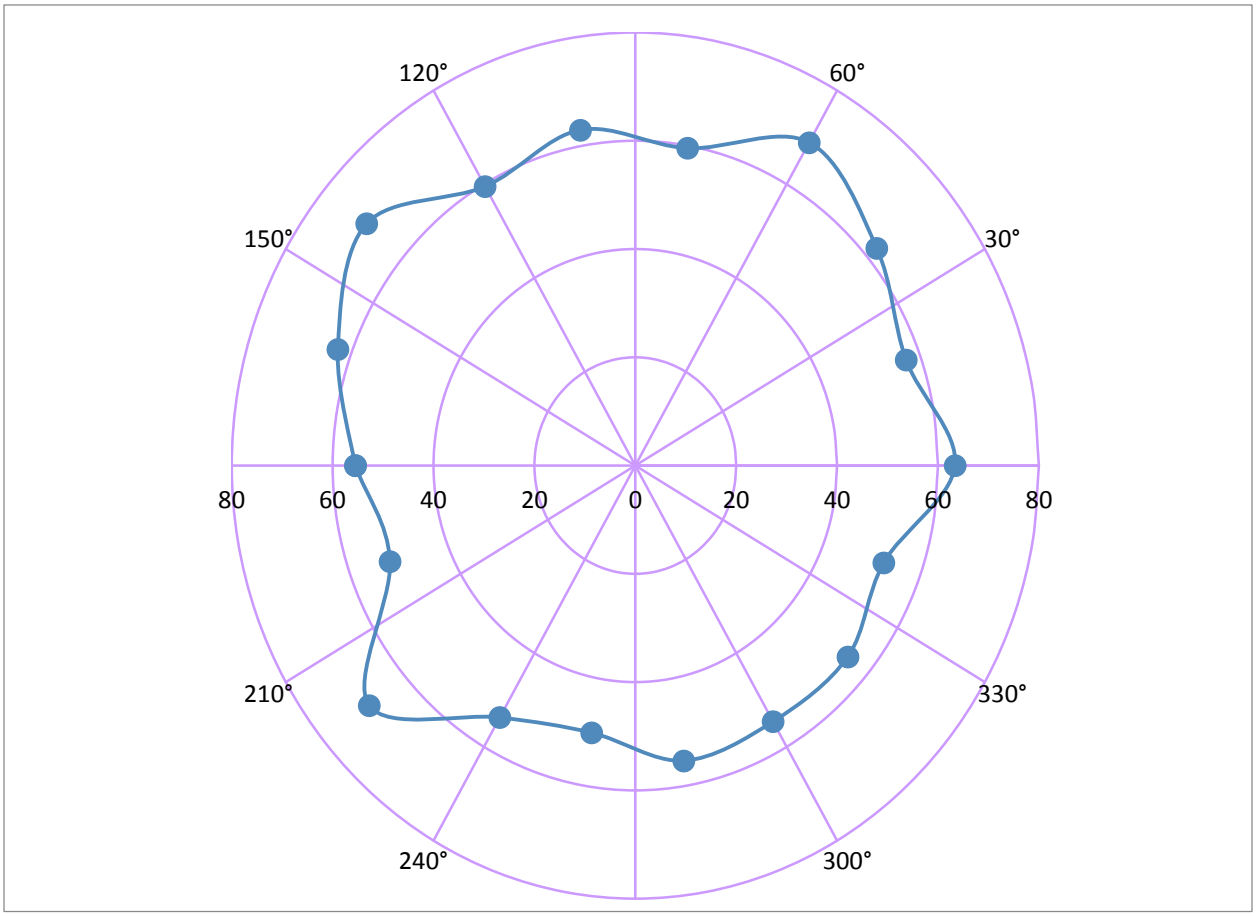

Figure 20. AUT2 Radiation pattern and measured received power

Angle [degree]	Ref Rx Power from AUT 3 [dBm]
0	-42.12
20	-51.56
40	-39.97
60	-38.7
80	-57.62
100	-40.78
120	-52.79
140	-50.77
160	-52.88
180	-62.96
200	-51.76
220	-54.08
240	-48.19
260	-41.67
280	-47.91
300	-40.94
320	-34.98
340	-38
360	-42.12

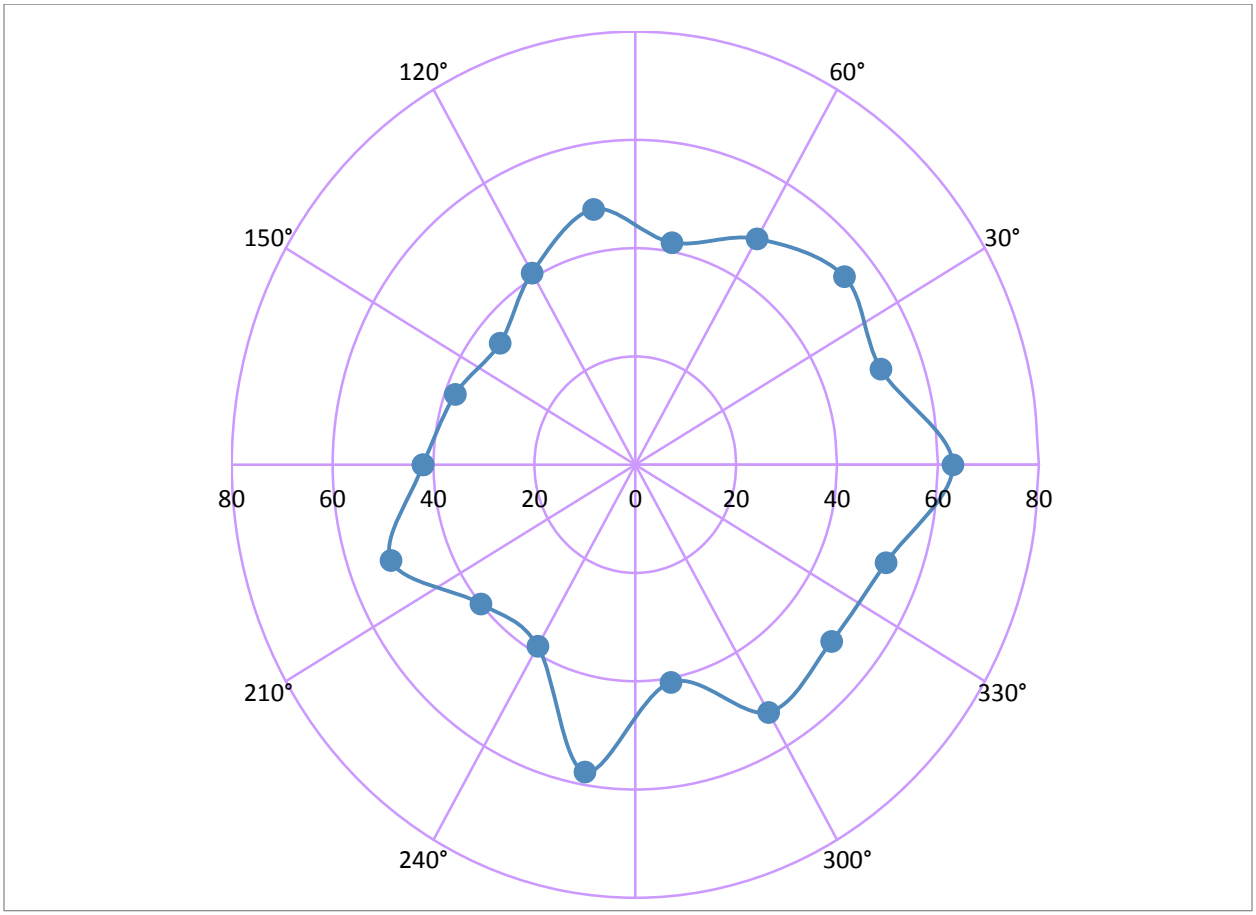

Figure 21. AUT3 radiation pattern and measured received power

From figures 19 and 21, both radiation patterns are similar since both antennas are based around the same coupled loop design. AUT 2 has a much more circular radiation pattern as seen in Figure 18.

5. Efficiency

Efficiency is calculated using measurements that we've already collected. The gain of the transmitting reference antenna is 1.8dBi, and the signal is 1dBm. The required data for calculation is shown in Table 3 below.

	AUT1	AUT2	AUT3
S11 (Γ) [dB]	-5.722	-2.346	-3.476
Received power [dBm]	-43.66	-58.9	-38
Received power [nW]	279	1.3	158
Reflected Power [%]	7.2	33.9	20.2
gain [dBi]	13.656	10.985	13.365
pathloss [dB]	-48.1	-45.5	-47.9
pathloss [nW]	-78.1	-75.5	-77.9

Table 3. Measured power parameters for efficiency calculation

$$P_{out} = P_{TX} + G_{ref} = 1dBm + 1.8dBi = 2.8dBm$$
$$P_{65cm} = P_{out} - PF = 2.8dBm - 48.1dBm = -45.3dBm = 3nW$$
$$P_{in} = \frac{P_{recieved}}{1 - \%refected} = \frac{279e^{-9}}{1 - 7.2\%} = \frac{279e^{-9}}{92.8\%} = 300.6nW$$
$$\eta = \frac{P_{out}}{P_{in}} = \frac{3nW}{300nW} = 1\%$$

	Efficiency
AUT1	1%
AUT2	Less than 1%
AUT3	15.6%

Table 4. Summary of tested antenna efficiency

Our tested efficiency does for AUT2 and AUT3 is close to the theoretical values from our simulation for Design 1 and 2. On the other hand, AUT1 fails to meet the expected efficiency because it was not properly tuned to 2.4GHz during the test. The outer ring needed to be shorted by scrubbing off the silver. Due to time constraints and failed attempts, we had to make due with testing a close to-but-not-perfect antenna.

Contact Angle Testing

Contact angle testing was used to primarily determine the wettability of the surface of PDMS, the exterior component of the final lens design. The materials used for this test included a sample of PDMS encased PET (the finals lens, *sans* circuitry,) a VCA Optima contact angle system, saline, and DI water. Figure 22 below depicts this test in progress.

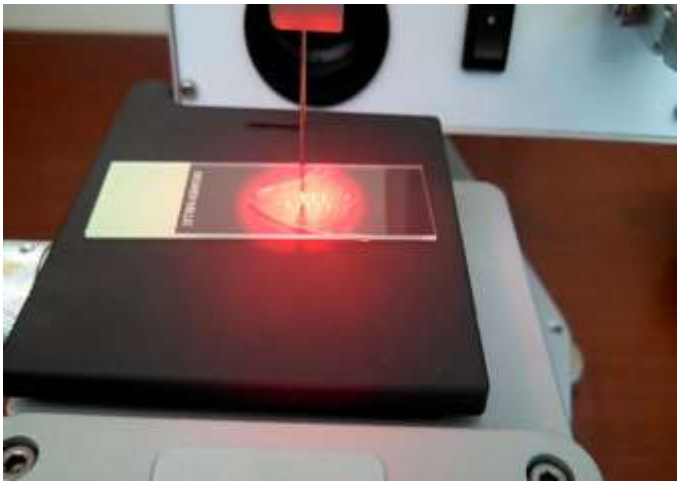

Figure 22: Contact angle test in progress using VCA Optima system.

The results of these tests were very clear: PDMS is not nearly hyrophonic enough to provide a comfortable, clear adhesion of the prototype lens to the human eye. Contact lenses rely on the surface tension created by the tear layer between the eye and the lens to remain in place. If a material with insufficient wettability is placed on the eye, the tear layer will glob up and areas of the lens will be in direct contact with the eye, causing irritation and blurry vision. Results from this test were computed and are presented in figure 23 below.

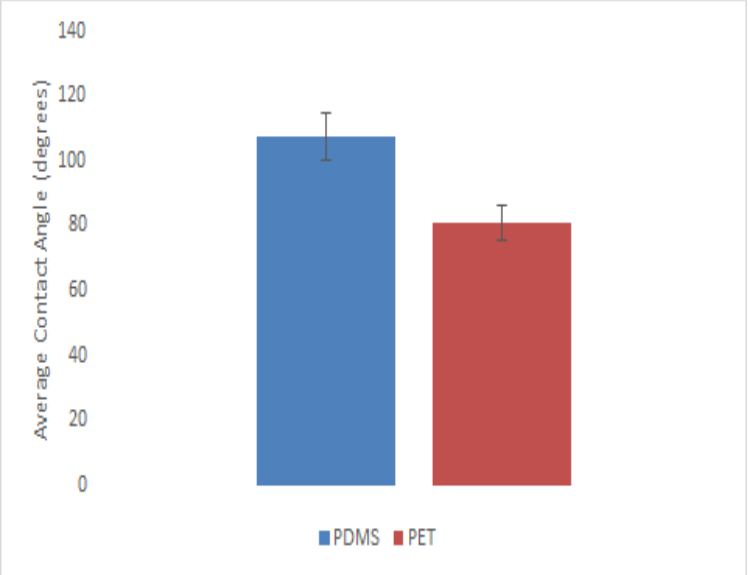

Figure 23: Bar chart of average contact angles for PET and PDMS, including standard error bars. (n = 15)

As can be seen in the figure above, PDMS has a contact angle of around 105^{o}, far exceeding the upper limit of 65^{o} set in the final specification. The most straightforward way to remedy this large contact angle would be the use of a surface hydrogel coating for contact lens. Silicone hydrogels are contemporary materials developed in 1999 to solve the problem of contact lens induced ocular hypoxia. They are highly permeable, and have a desirable contact angle for use in contact lens applications. Traditionally, they are cut using a lathe from a solid

block of material. This would make applying to the surface of PET difficult. Recently, however, a patent filed under the number WO2009073401 A2 proposes the creation of a novel silicon hydrogel spray for use in tissue dressing application [20]. Should this technology come to fruition, it would be an excellent substitute for PDMS as an exterior lens material.

Comfortability

Biocompatibility Assessment

The purpose of biocompatibility assessment was to determine whether the final design improved upon previous designs which exposed PET to the surface of the eye. PET, as stated in our preliminary analysis, has been shown to yield endocrine disruptive properties. Additionally, PET is traditionally characterized a “hard” contact lens material, with a high elastic modulus and characteristically rough surface. This makes PET fairly uncomfortable when placed on the human eye for long periods of time. In our final design, we purposely encapsulated PET with PDMS to circumvent some of the uncomfortable aspects of PET with a softer, more flexible polymer. An illustration of this design is shown in figure 24 below.

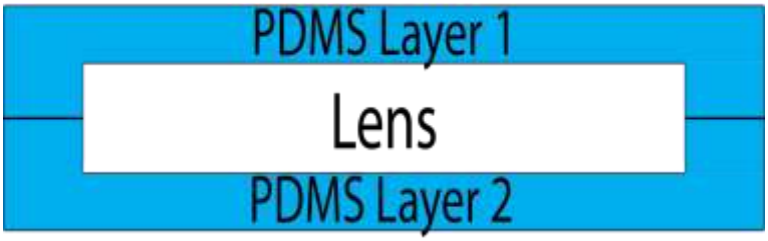

Figure 24: PET lens base completely encapsulated by PDMS. In general, layer one is much thicker than layer two.

We define a material as biocompatible when it a) does no harm to the human body and b) when the human body does no harm to it. While this definition appears archaic, it is the first requirement that is of utmost importance. Irritation, hypoxia, and hormonal disruption are all undesirable and would readily fall under the definition of “harmful” in our scenario. After surveying tissue engineering literature, it was determined that PDMS is readily used in biological scenarios and displays biocompatible qualities both *in vitro* [21] and *in vivo* [22]. Thus we can conclude that it is suitable in preventing long term exposure to PET in physiological temperatures. To strengthen this conclusion, *in vitro* assessment can be performed over a long period of time to determine cell adhesion and cell toxicity properties. The former would involve colonizing cells on the surface of substrate material and attempting to wash cells off at various time points. The number of cells remaining versus the number of cells washed away can be used as a metric for cell adhesion. The latter would involve placing a layer of agar over a pre colonized layer of cells, and placing a layer of PDMS above the agar, allowing the PDMS to diffuse slowly into the cell layer. Microscopy to examine cell death could then be used as a metric for cellular toxicity *in vitro*.

Thickness Testing

The total thickness of the prototype was determined using calipers accurate to 3/1000th's of an inch. The primary goal of this test was to verify that the after the overall manufacturing process was completed, the lens thickness remained within the desired specification. This test was performed knowing that the thickness of the final design would greatly exceed the planned specification due to time and cost constraints. To account for variability in thickness over the surface of the lens, 15 separate points were chosen for thickness measurements. Figure 25 below contains the materials used in this test.

Figure 25: Materials used to characterize thickness of manufactured substrate and prototype.

From this test, it was determined that the overall thickness of the lens was about 800 microns with a standard error of 71.12 microns (n = 15.) As stated before, this far exceeds the desired specification of 400 microns. The solution to this is a much smaller integrated circuit fabrication process to achieve smaller feature sizes and an overall thinner integrated circuit. This, ideally, would bring overall thickness down to around 450 microns.

Substrate Breathability Testing

As with biocompatibility, quantifying substrate breathability is difficult without expensive equipment and large amounts of time. Systems built to determine the permeability of a material to oxygen, such as the LabThink OX2/231 Oxygen Permeability Tester, are not readily available for students and are designed for industrial lab usage. As such, the primary means of verifying oxygen permeability for our substrate materials was through a survey of literature and research on polymer oxygen permeability.

While PET is not permeable to oxygen whatsoever (a property which has earned it a throne in the plastic bottling industry,) PDMS has a very high oxygen permeability at physiological temperature [23]. Since PDMS encapsulates the PET and subsequently the lens, oxygen can readily diffuse throughout the exterior layer and circumvent the PET boundary. Additionally, areas which are covered by PET but do not contain any functional components can potentially be removed in future iterations of the device, further improving oxygen permeability of the lens. In order to strengthen information obtained in these surveys, simulations in

COMSOL can be performed to determine transient oxygen concentration on the ocular side of the lens. These simulations, however, are not straightforward, and require large amounts of data regarding nonlinear oxygen metabolism of ocular tissue as well as diffusion coefficients for ocular tissues. Further complexity is introduced when considering the air layers between the PET and PDMS.

Bioheat Analysis

Further bioheat analysis was performed via simulations in COMSOL by introducing a nonlinear conductivity model for ocular tissue with thermally significant vessels. This method was first described by Weinbaum *et al*. in a landmark study on the effects of blood flow on local average tissue temperature [24]. In this method, tissues that are perfused with blood experience a nonlinear increase in conductivity, which creates “resistance” to heat flow into the tissues. A surface plot of the temperature distribution using this model is shown in figure 27 below.

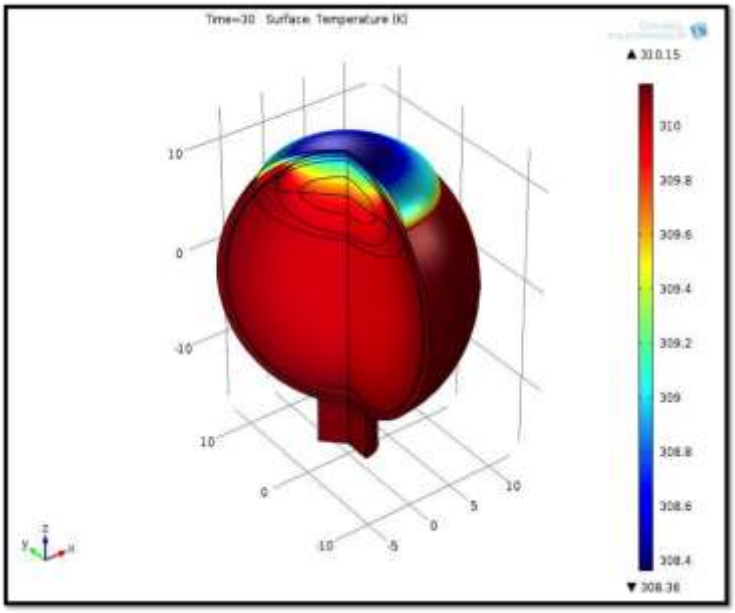

Figure 27: Nonlinear conductivity bioheat model transient temperature analysis.

The most significant observation of this result is its similarity to the previous model’s result. Using simply the Penne bioheat equation, a nearly identical temperature distribution was achieved in preliminary analysis. There are a few likely causes for this similarity. The first cause is the presence of a large artery at the bottom of the model that acts as an outflow condition. When microvasculature is in close proximity to the large vessel, such as the one shown above, the Penne bioheat equation tends to dominate, as the large vessel acts as a heat sink for which excess thermal energy can exit the system. While a microvascular model was implemented in the domain of the Iris near the cornea, the effect of the perfusion was minimal when compared to blood flow via the retinal arteries. The second is the difficulty associated with measuring microvascular perfusion rates in ocular tissues. Since the new model relies on using blood perfusion in tissue to calculate new values of thermal conductivity, a constant value of perfusion

for each tissue is not sufficient. The value must be dynamic, based upon available experimental data of transient blood flow in the human eye. In the time our team had to create and use this model, developing such a realistic simulation of ocular blood flow was not feasible.

IX Impact, Conclusion, and Recommendations

At the onset of the Clear Active Contact Lens project, our group set out to do four things: modify the project to include a medical perspective, establish a quantitative set of design requirements based on this new perspective, develop a robust and safe process for manufacturing the new product, and test and evaluate our products biomedical requirements. We looked to previous designs and attempts at creating an active contact lens and ask ourselves “how can we improve that, and if we can, how do we know it’s an improvement?” At the end of the road, with a prototype in hand, it is safe to say that we have successfully created a platform for an active contact lens that makes the device more sustainable, isolated, and safe. We believe that the combination of biomedical ingenuity and novel functionality associated with our design sends a strong message to future groups of students looking to make active contact lenses. Our acceptance into the Engineering in Medicine and Biology Conference in Chicago, Illinois, as well as the feedback from our sponsor confirms that our work has made a definitive impact on the cutting edge research of active contact lenses.

At this point, we hope that future teams will take this work as a reference for the embedding of a functional platform into a contemporary contact lenses. There is still much work that needs to be done to ensure that our design meets the high standard set by the FDA for medical devices. Our heartfelt recommendation is that the work we performed in verifying the biomedical requirements of the device are improved upon, such that the device can one day be examined for *in vivo* and clinical study. Active contact lenses represent a milestone in communicating visual information to an increasingly diverse and technically apt population. It is our desire to see a device similar to ours one day contributing to the overall safety of the population.

Appendix A - Senor Project Analysis

1. Summary of Function Requirements

This project functions as a research and development stepping stone for future works in active contact lens. It lays the groundwork for a manufacturing process of PET and PDMS lens that are clear and comfortable. The IC design is a basis for signal processing and charge control at for nano size devices. The antenna provides a stepping stone for effective and efficient signal transfer at a millimeter scale as well as an attempt at wireless power transfer. The battery research is an ongoing effort to produce a nonhazardous, flexible, and long lasting power source for the contact lens. This proof of concept is one great leap towards a future technology.

2. Primary Constraints

The first requirement we could gather was that the lens needed to be clear. Our initial target customer base is largely situated in hazardous waste control. In this occupation, unclouded vision is absolutely necessary. The individual must be completely aware of what is in front of them and around them through the use of visual recognition, since environmental suits will obstruct other senses, such as smell, hearing, and touch. Another requirement is comfortability, since the individual will more than likely not be able to perform any field adjustments on the lens itself. This is by far one of the most difficult requirements to incorporate into device design. As such, any materials used will need to be inspected for minimal adverse reactions, with the most important being inflammation, when in contact with the body. Finally, the terminal requirement is isolated functionality. To remain competitive in the young market place of active wearable devices, the clear active contact lens must not require any input or command from the customer. The device must maintain autonomy from the user so that he or she can focus on the task at hand. When the device has meaningful data to provide, it will do so with a designated stimulus, in our case an LED. Otherwise, it will remain off and out of the way.

3. Economic

We hope to present our project at the EMBS conference (Engineering Medicine Biology Society of IEEE) in August 2014, BioCas, and ISSCC. We are also planning to submit our research to publications such as IEEE Journal of Biomedical and Health Informatics, IEEE Transactions on Biomedical Circuits and Systems, and IEEE Transactions on Consumer Electronics. There has not been much research regarding clear circuits for contact lens applications so our work would lay additional groundwork for future miniature circuit project. Table 3 shows our initial cost projections. Our final cost of everything is $2568.89, which includes $500 for CNC tech hours and materials, $1744.95 R&D graphene supercapacitor, and $323.94 Electrical components and thin film battery. Much of our thin film printing process was donated by the GrC department. A timeline of our project development is shown in Figure 1.

Supplier	Part Number	Description	Unit Price	Quantity	Total Price
Henkel	ECI 5001 E&C	Translucent Conductive Ink	$618 / 0.2kg	0.4kg	$1,236.00
GoodFellow	862-677-51	PMMA sheet 600x500mm 0.38mm thickness	$250/2sheet	2 sheets	$250.00
Enfucell	Mini 1.5V	1.5V printed battery. 0.7mm thickness	$0.50	20	$10.00
Minicircuits	PGA-105+	Monolithic RF Amp 15dB gain	$1.99	20	$39.80
Digikey	ML8511-00FCZ05B	UV Sensor w/ amp	$7.66	5	$38.30
Digikey	1N5711W-7-F	Schottky Diode	$0.44	10	$4.40
Digikey	MAX2750EUA+	2.4GHz VCO	$3.30	5	$16.50
Digikey	-	Resistors	$1.01	25	$25.25
Digikey	-	Capacitors	$0.34	25	$8.40
Digikey	511-1304-1-ND	Red SMT LED	0.2816	25	$7.04
IEEE		EMBS Conference Registration	$475	3	1425
Travel		Flight for EMBS Conference in Chicago	$389	3	$1,167.00
Hotel		Hotel for EMBS Conference in Chicago	$95	1	$95
				Total:	**$2,897.60**

Table 3. Cost Estimate

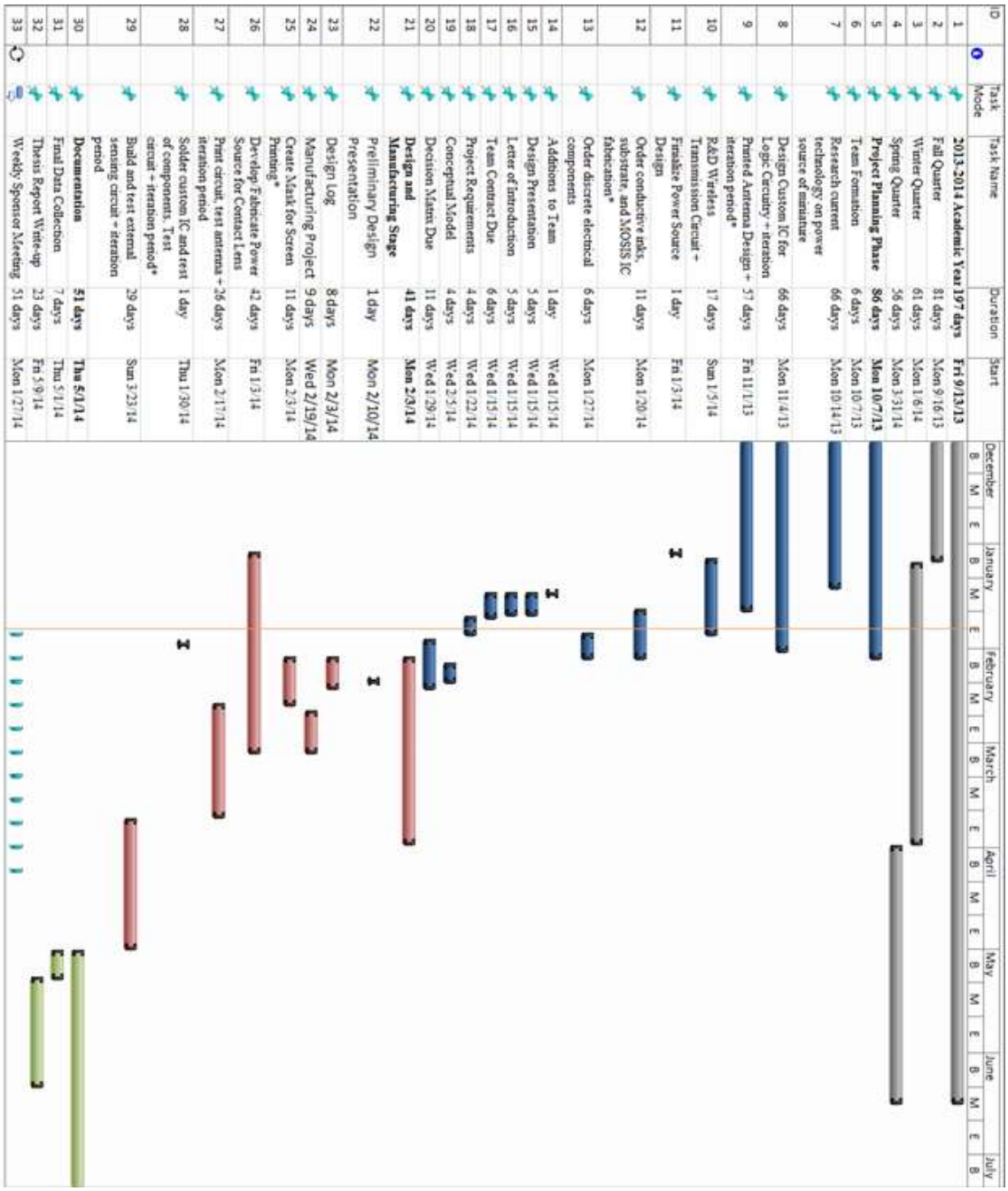

Figure 1: Updated Gantt chart to reflect most recent project status.

4. Environmental

The circuit uses translucent conductive ink printed on PET and PDMS sheet. These use natural resources that the manufacturers have not released as public information. The contact lens design has humans as the primary market and do not directly affect other species. Whether or not the manufacturers' of the components affect other species is not public knowledge.

5. Manufacturability

The lens manufacturing process was designed to be simple and robust. The process overview involves four major steps: printing the lens, curving the lens, attaching the components, and embedding the circuit in PDMS. To carry out this process, manufacturing techniques from across disciplines were used. Screen-printing machines in the GrC department were used to fabricate the antennas. The molds were designed using SolidWorks in the BMED computer lab and manufactured in the Bonderson Machine shop. The PDMS was mixed and degassed using the Micro fabrication lab facilities.

Outline of Manufacturing Process

1. Screen Print Antenna
2. Attach PET Substrate to Male Mold 1
3. Place Mold in oven at 180 degrees Celsius for 10 minutes
4. Attach components using thermo-epoxy
5. Use Mold 2 to build top layer of PDMS
6. Use Mold 3 to build bottom layer of PDMS

6. Sustainability

The contact lens is not a sustainable product and would not last longer than the life of the printed battery. Future improvements to the design include additional sensors, transparent transistors, more efficient antenna, and more pixels than a single LED. Because of the size constraint, any upgrade to the design will reduce some existing aspect unless smaller components are invented. Practicality of contact lens also requires transparency, which is not feasible with some hardware. Health issues with being in direct contact with the eye also constrains the heat, chemical, and radiation effects of the circuit design.

7. Ethical

This design has the user's health as the highest priority. All specifications and possible side effects of use of the contact lens will be disclosed with 100% transparency. We will anticipate hazards and design safety measures. This project will be presented at EMBS conference to share our design with other professionals in the printed electronics field.

8. Health and Safety

As a product that is in contact with the eye, safety is our top concern. The contact lens material is designed to a sufficient degree of clearness for unimpaired visibility, flexibility for a non-irritable wear, biocompatibility to prevent harm to the eye. We've simulated the heat dissipation at the peak of power consumption of the IC and confirmed its safety.

9. Development

This project has pushed thin film printing technology to being able to print fine line designs of 250μm. We have also streamlined the mold process of the materials.

Appendix B - References

References

[1] "Fatal Occupational Injuries in 2012 - Chart Package." Occupational Health and Safety Administration. U.S. Department of Labor, 2012. Web. 20 Jan. 2014.

[2] Lingley, Andrew R., et al. "A single-pixel wireless contact lens display." Journal of Micromechanics and Microengineering 21.12 (2011): 125014.

[3] J. Pandey, Y. Liao, and A. Lingley, “A fully integrated RF-powered contact lens with a single element display,” *… Circuits Syst. …*, vol. 4, no. 6, pp. 454–461, 2010.

[4] B. Parviz, “For your eye only,” *Spectrum, IEEE*, no. september 2009, pp. 36–41, 2009
[5] H. Yao, A. J. Shum, M. Cowan, I. Lähdesmäki, and B. a Parviz, “A contact lens with embedded sensor for monitoring tear glucose level.,” *Biosens. Bioelectron.*, vol. 26, no. 7, pp. 3290–6, Mar. 2011.

[6] A. Kagie, D. K. Bishop, J. Burdick, J. T. La Belle, R. Dymond, R. Felder, and J. Wang, “Flexible Rolled Thick- Film Miniaturized Flow- Cell for Minimally Invasive Amperometric Sensing,” *Electroanalysis*, vol. 20, no. 14, pp. 1610–1614, Jul. 2008.

[7] S. Iguchi, H. Kudo, T. Saito, M. Ogawa, H. Saito, K. Otsuka, A. Funakubo, and K. Mitsubayashi, “A flexible and wearable biosensor for tear glucose measurement.,” *Biomed. Microdevices*, vol. 9, no. 4, pp. 603–9, Aug. 2007.

[8] P. C. Nicolson and J. Vogt, “Soft contact lens polymers: an evolution.” *Biomaterials*, vol. 22, no. 24, pp. 3273–83, Dec. 2001.

[9] "Medical Devices." *Radio Frequency Wireless Technology in*. FDA, 13 Aug. 2013. Web. 26 Jan. 2014.

[10] Naoki Sadayori and Yuji Hotta "Polycarbodiimide having high index of refraction and production method thereof" US patent 2004/0158021 A1 (2004)

[11] L. B. Kish, "End of Moore's Law: Thermal (Noise) Death of Integration in Micro and Nano Electronics," Phys. Lett. A. **305** 144 (2002).

[12]Gokul, K. C., D. B. Gurung, and P. R. Adhikary. "Effect of Blood Perfusion and Metabolism in Temperature Distribution in Human Eye." Advances in Applied Mathematical Biosciences 4.1 (2013): 13-23.

[13] Cvetkovic, Mario, Dragan Poljak, and Andres Peratta. "Thermal modelling of the human eye exposed to laser radiation." Software, Telecommunications and Computer Networks, 2008. SoftCOM 2008. 16th International Conference on. IEEE, 2008.

[14] Liu, Chenguang, Zhenning Yu, David Neff, Aruna Zhamu, and Bor Z. Jang. "Graphene-Based Supercapacitor with an Ultrahigh Energy Density." *Nano Letters* 10.12 (2010): 4863-868. Print.

[15] "Graphene." *Wikipedia*. Wikimedia Foundation, 25 Jan. 2014. Web. 27 Jan. 2014.

[16] S.J. Wang, Y. Geng, Q. Zheng and J.k. Kim, "Fabrication of highly conducting and transparent graphene films," Carbon, 48, 1815–1823 (2010).

[17]Leonard Sax (2010). "Polyethylene Terephthalate May Yield Endocrine Disruptors". Environmental Health Perspectives 118 (4): 445–8.

[18] R.M. Ford and C.S. Coulston, *Design for Electrical and Computer Engineers,* McGraw-Hill, 2007.

[19] El-Kady, Maher. "Laser Scribing of High-Performance and Flexible Graphene-Based Electrochemical Capacitors - Supporting Online Material." *Laser Scribing of High-Performance and Flexible Graphene-Based Electrochemical Capacitors - Supporting Online Material*. Science Magazine, 16 Mar. 2012. Web. 3 Nov. 2013.

[20] McCrea, Keith R., Yuan Tian, and Robert S. Ward. "Silicone hydrogels for tissue adhesives and tissue dressing applications." U.S. Patent Application 12/745,509.

[21] Seitz, Helmut, et al. "Biocompatibility of polyethylene terephthalate (Trevira< sup>®</sup> hochfest) augmentation device in repair of the anterior cruciate ligament." Biomaterials 19.1 (1998): 189-196.

[22] Seitz, H., et al. "Biocompatibility of polyethylene terephthalate--PET--(Trevira strong)--an in vivo study of the sheep knee." Biomedizinische Technik. Biomedical engineering 41.6 (1996): 178.

[23] 10] Merkel, T. C., et al. "Gas sorption, diffusion, and permeation in poly (dimethylsiloxane)." Journal of Polymer Science Part B: Polymer Physics 38.3 (2000): 415-434.

[24] Weinbaum, S., and L. M. Jiji. "A new simplified bioheat equation for the effect of blood flow on local average tissue temperature." Journal of biomechanical engineering 107.2 (1985): 131-139.

[24]"Flat Spiral Coil Design Calculator." *Flat Spiral Coil Design Calculator*. Circuits, 9 Dec. 2010. Web. 27 Jan. 2014.

Appendix C - Final Drawings

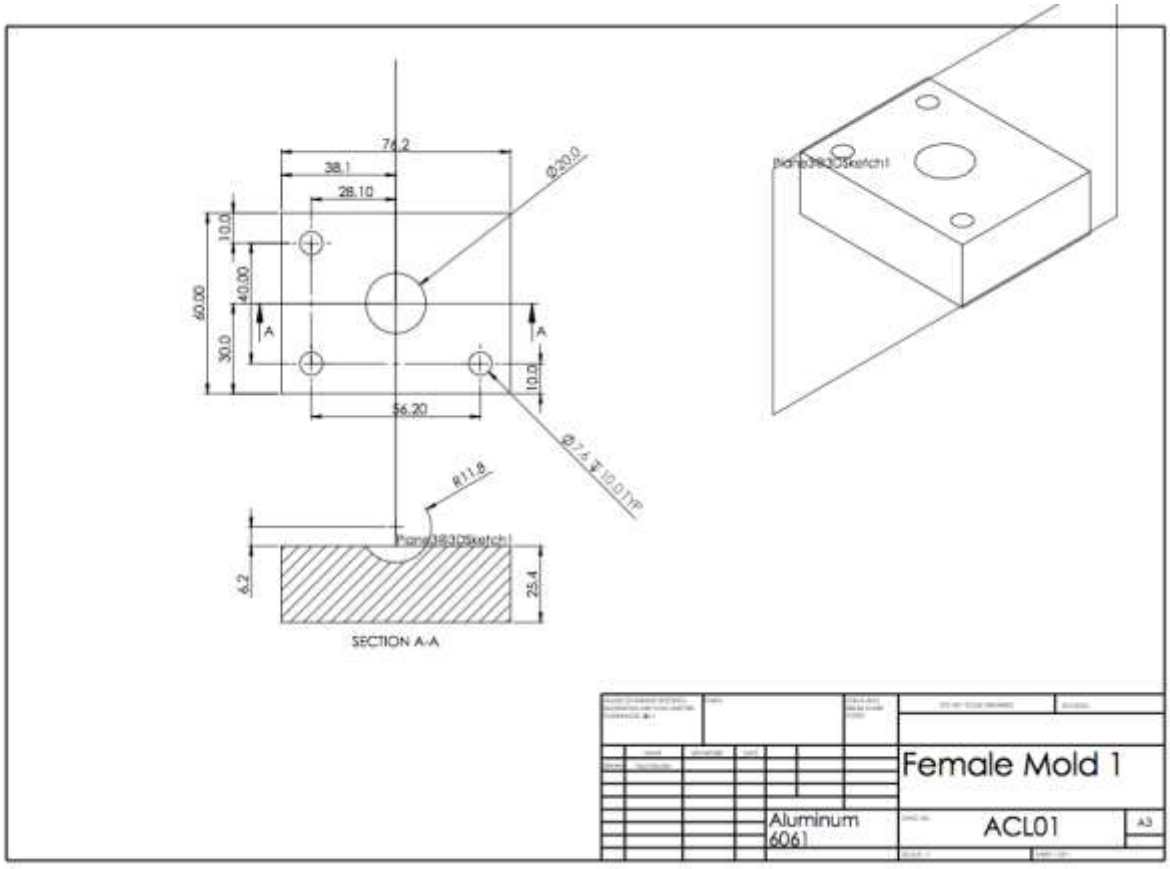

Figure 1: Drawing of Female Mold 1

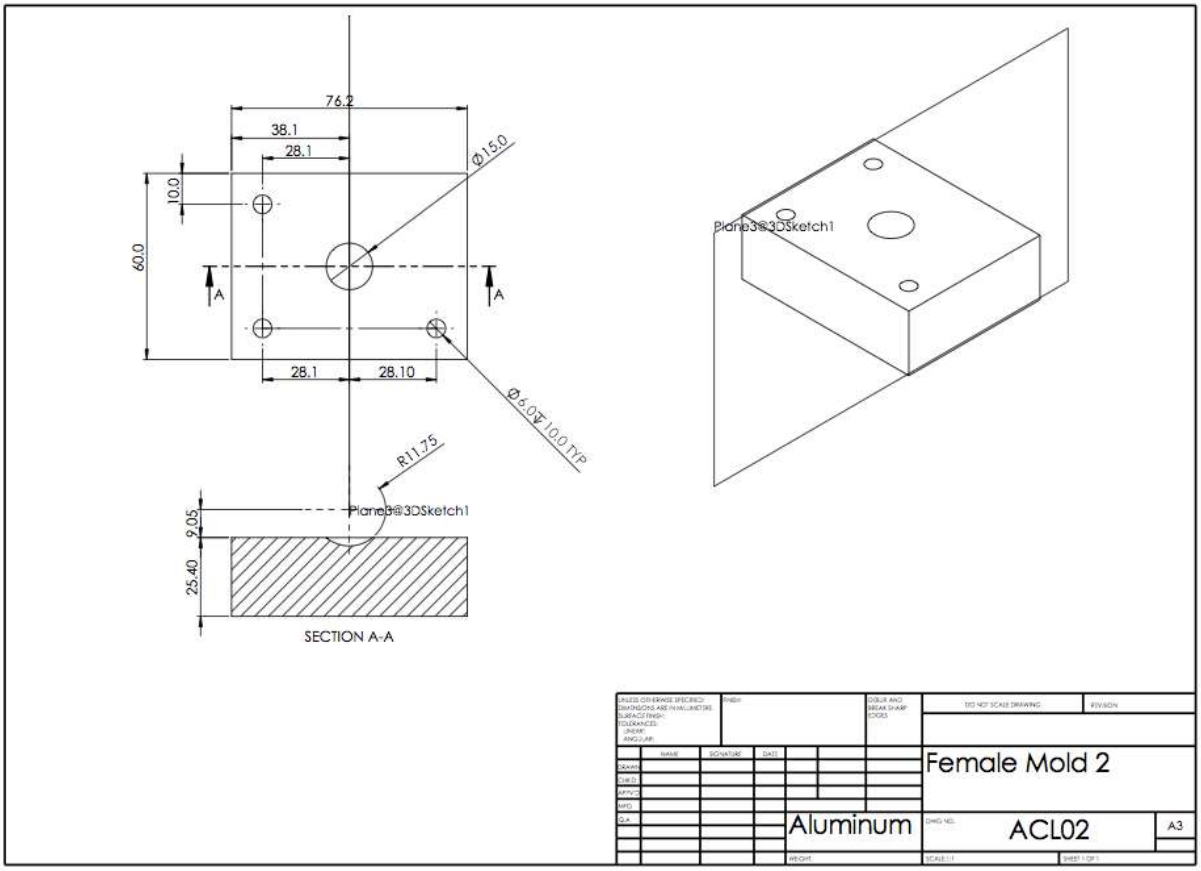

Figure 2: Drawing of Female Mold 2.

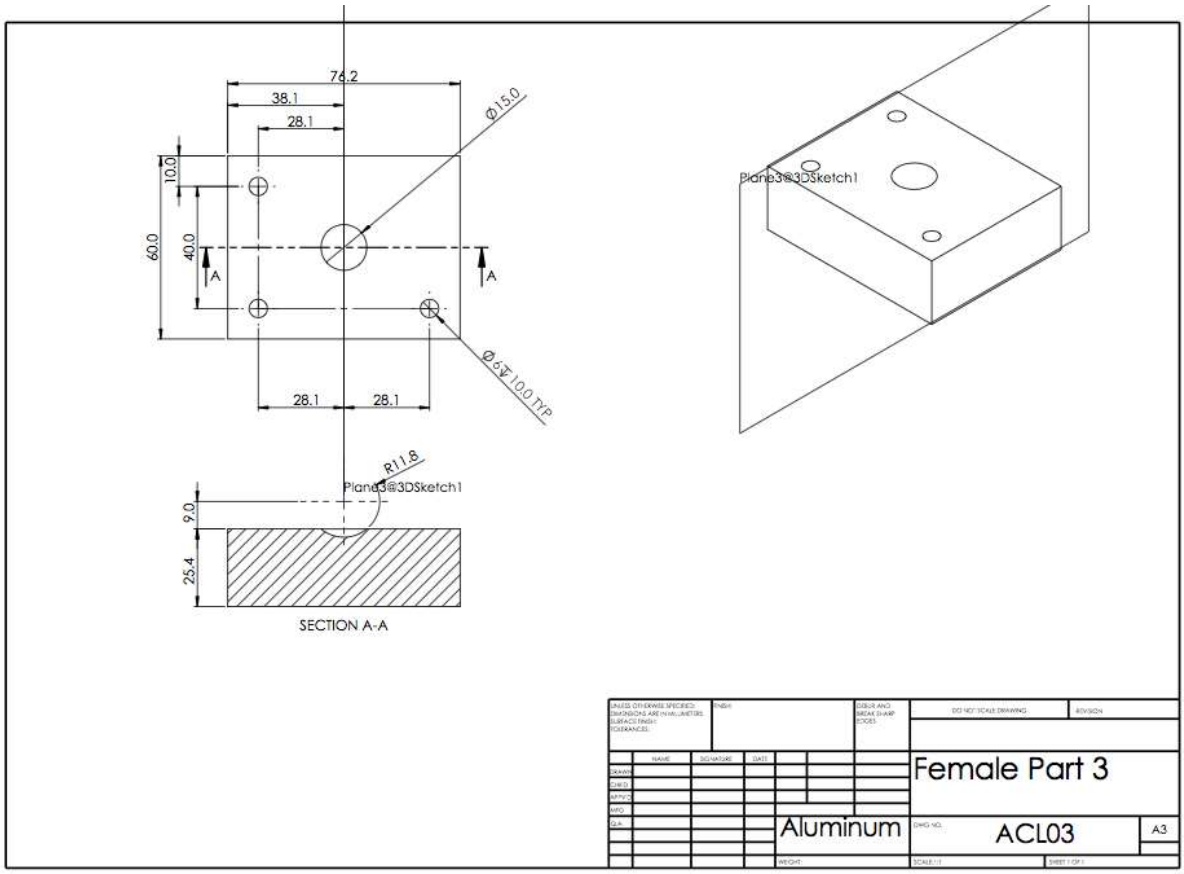

Figure 3: Drawing of Female Mold 3.

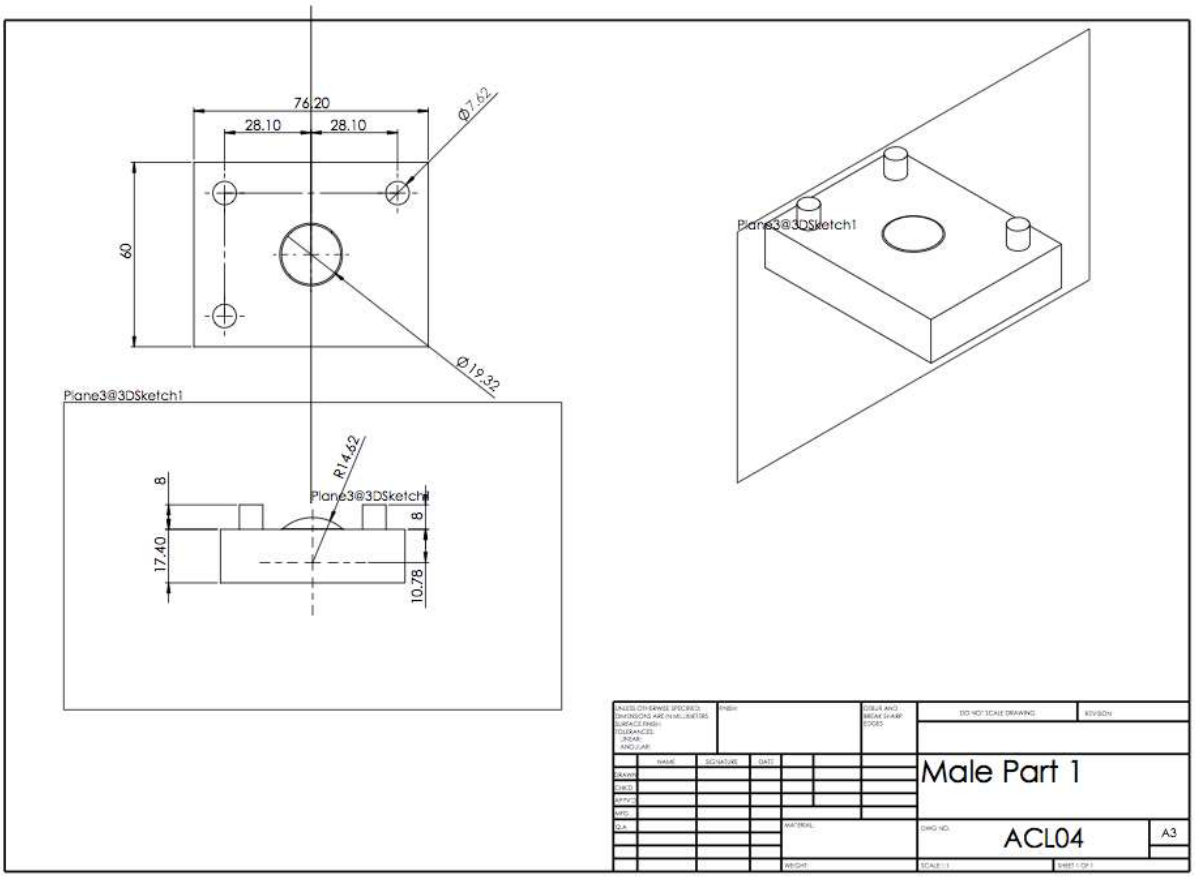

Figure 4: Drawing of Male Mold 1.

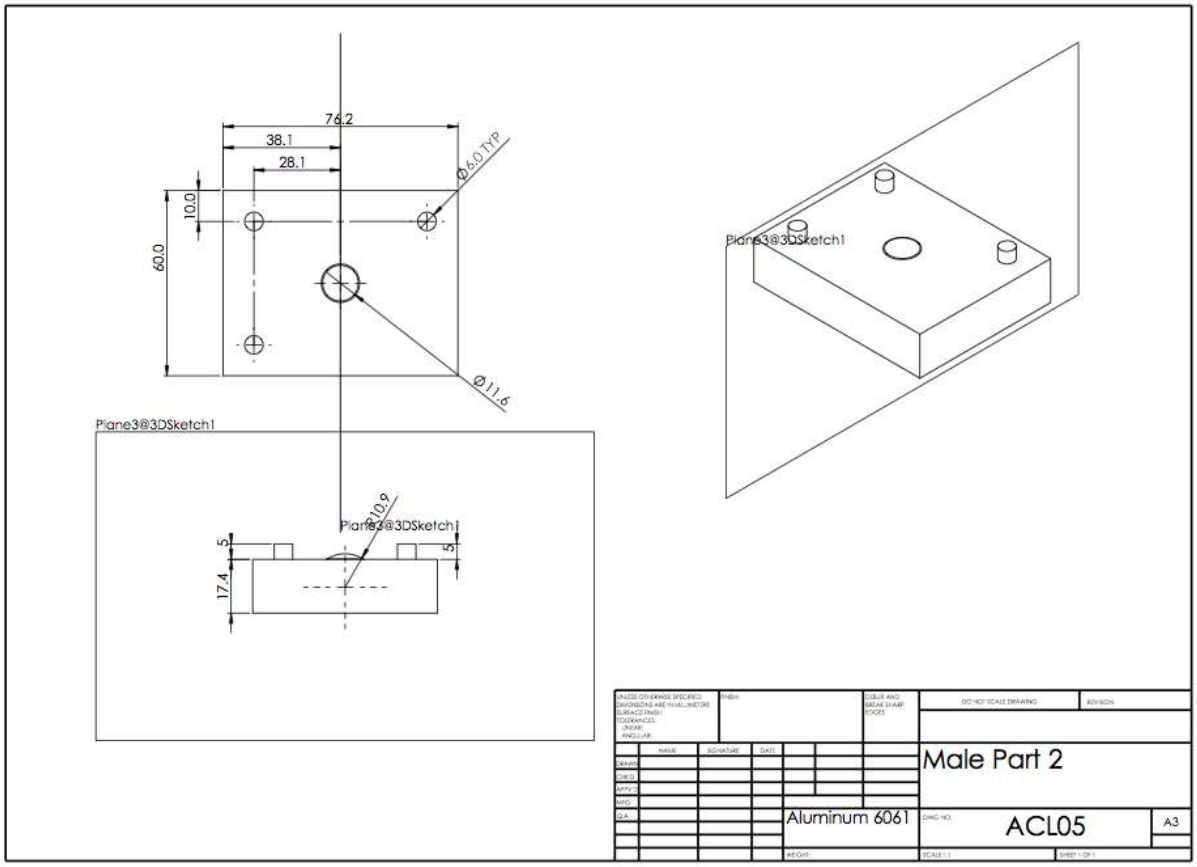

Figure 5: Drawing of Male Mold 2.

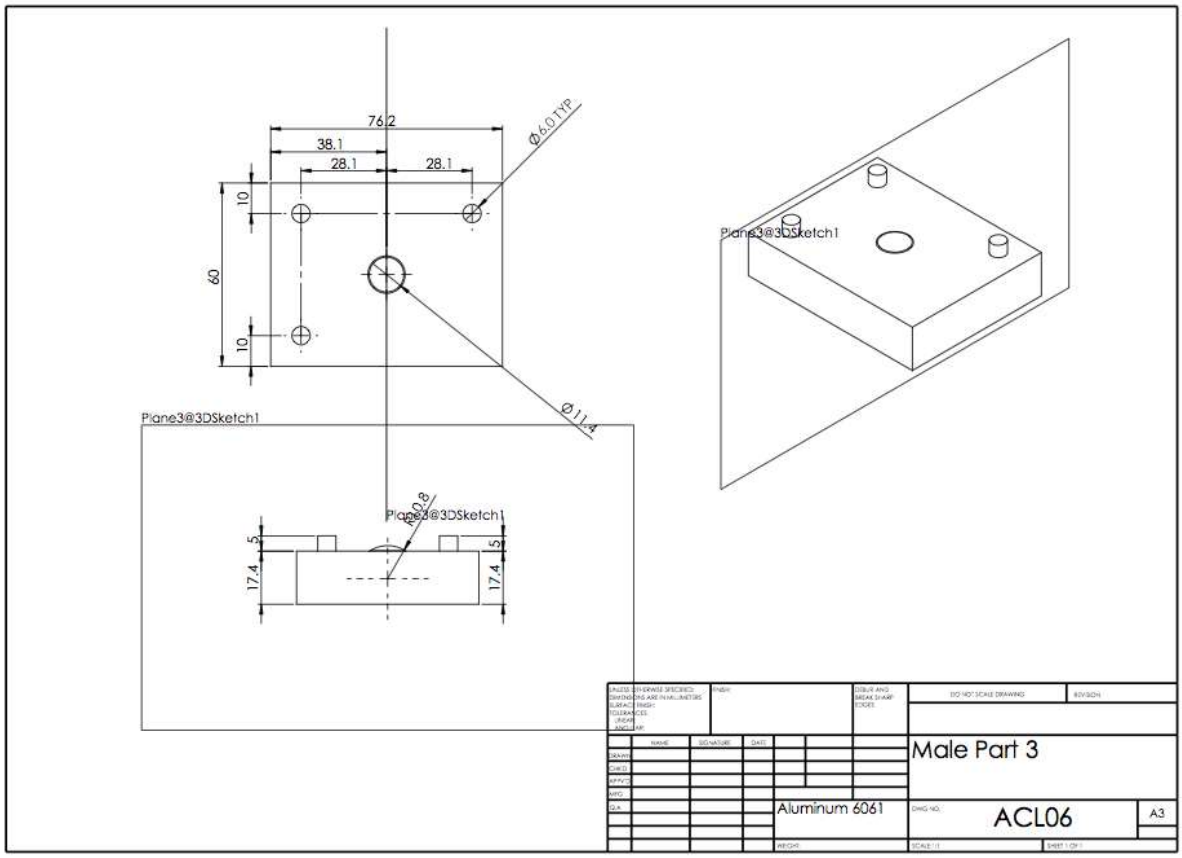

Figure 6: Drawing of Male Mold 3.

Appendix D - List of Vendors, Contact Information, Pricing

- Cymbet CBC005 Thin Film battery: Qty = 143, Total Cost = $250
  Cymbet™ Corporation, 18326 Joplin Street NW, Elk River, MN, 55330-1773
  Phone: 763.633.1780

- Rohm Semiconductor Red LED: Qty = 10, Total cost = $4.20
- Rohm Semiconductor ML8511 UV Sensor: Qty = 5, Total Cost = $38.30
  ROHM Semiconductor U.S.A.,LLC
  6020 Cornerstone Court West, Suite 320, San Diego, CA 92121 U.S.A.
  TEL : +1-858-625-3600 FAX : +1-858-625-3640

- Fairchild MMG3002MT1 RF amplifier: Qty = 3, Total Cost =$14.94
  Fairchild Semiconductor Corporation
  3030 Orchard Parkway
  San Jose, CA 95134
  U.S.A.
  Tel: 408-822-2000

- Maxim MAX2750EUA+ 2.4GHz oscillator: Qty = 5, Total Cost = $16.50
  Corporate Headquarters
  Maxim Integrated
  160 Rio Robles
  San Jose, CA 95134 USA
  408-601-1000

- One Industrial Way
  2705 McMillan Ave, San Luis Obispo, CA 93401
  (805) 596-0645

1x 1/2" carbide, 3 flute, flat end mill for aluminum (estimate ~$30ea)

1x 1/4" carbide, 3 flute, flat end mill for aluminum (estimate ~$25ea)

2x 1/8" carbide, 3 flute, flat end mill for aluminum (estimate ~$20ea)

2x 1/8" carbide, 3 flute, ball end mill for aluminum (estimate ~$15ea)

2x 1/16" carbide, 3 flute, ball end mill for aluminum (estimate ~$15ea)

- McMaster Carr
  9630 Norwalk Blvd.
  Santa Fe Springs, CA 90670-2932
  (562) 692-5911

1	8975K239	Multipurpose 6061 Aluminum, 1" Thick X 3" Width X 1' Length	2 each	today	24.34 each		48.

CYMBET™ CORPORATION

EnerChip™ CBC050

Rechargeable Solid State Energy Storage: 50µAh, 3.8V

Features

- All Solid State Construction
- SMT Package and Process
- Lead-Free Reflow Tolerant
- Thousands of Recharge Cycles
- Low Self-Discharge
- Eco-Friendly, RoHS Compliant

8 mm x 8 mm
QFN SMT Package

5.7 mm x 6.1 mm
Bare Die

Electrical Properties

Output voltage:	3.8V
Capacity (typical):	50µAh
Charging source:	4.00V to 4.15V
Recharge time to 80%:	20 minutes
Charge/Discharge cycles:	>5000 to 10% DOD

Physical Properties

Package size:	8 mm x 8 mm
Operating temperature:	-20°C to 70°C
Storage temperature:	-40°C to 125°C

Applications

- **Standby supply** for non-volatile SRAM, real-time clocks, controllers, supply supervisors, and other system-critical components.
- **Wireless sensors and RFID tags** and other powered, low duty cycle applications.
- **Localized power source** to keep microcontrollers and other devices alert in standby mode.
- **Power bridging** to provide backup power to system during exchange of main batteries.
- **Energy Harvesting** by coupling the EnerChip with energy transducers such as solar panels.
- **Embedded Energy** where bare die can be embedded into modules or co-packaged with other ICs.

Pin Number(s)	Description
1	V+
4	V-
2,3	NIC
5-16	NIC
Note: NIC = No Internal Connection	

The EnerChip™ CBC050 is a surface-mount, solid state, rechargeable energy storage device rated for 50µAh at 3.8V. It is ideal as a localized, on-board power source for SRAMs, real-time clocks and microcontrollers which require standby power to retain time or data. It is also suitable for RFID tags, smart sensors, and remote applications which require a miniature, low-cost, and rugged power source. For many applications, the CBC050 is a superior alternative to coin cell batteries and supercapacitors.

Because of their solid state design, EnerChip™ storage devices are able to withstand solder reflow temperatures and can be processed in high-volume manufacturing lines similar to conventional semiconductor devices. There are no harmful gases, liquids or special handling procedures, in contrast to traditional rechargeable batteries.

The EnerChip recharge is fast and simple, with a direct connection to a 4.1V voltage source and no current limiting components. Recharge time is 20 minutes to 80% capacity. Robust design offers thousands of charge/discharge cycles. The CBC050 is packaged in an 8 mm x 8 mm quad flat package. It is available in reels for use with automatic insertion equipment.

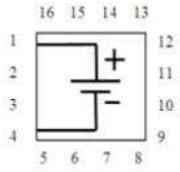

CBC050 Schematic - Top View

Operating Characteristics

Parameter		Condition	Min	Typical	Max	Units
Discharge Cutoff Voltage		25°C	3.0[1]	-	-	V
Charge Voltage		25°C	4.0[2]	4.1	4.3	V
Pulse Discharge Current		25°C	300[3]	-	-	µA
Cell Resistance (25° C)		Charge cycle 2	-	750	2000	Ω
		Charge cycle 1000	-	4200	7000	
Self-Discharge (5yr average; 25° C)		Non-recoverable	-	2.5	-	% per year
		Recoverable	-	1.5[4]	-	% per year
Operating Temperature		-	-20	25	+70	°C
Storage Temperature		-	-40	-	125[5]	°C
Recharge Cycles (to 80% of rated capacity; 4.1V charge voltage)	25° C	10% depth-of-discharge	5000	-	-	cycles
		50% depth-of discharge	1000	-	-	cycles
	40° C	10% depth-of-discharge	2500	-	-	cycles
		50% depth-of-discharge	500	-	-	cycles
Recharge Time (to 80% of rated capacity; 4.1V charge voltage)		Charge cycle 2	-	20	35	minutes
		Charge cycle 1000	-	60	95	
Capacity		100µA discharge; 25°C	50	-	-	µAh

(1) *Failure to cutoff the discharge voltage at 3.0V will result in EnerChip performance degradation.*

(2) *Charging at 4.0V will charge the cell to approximately 70% of its rated capacity.*

(3) *Typical pulse duration = 20 milliseconds.*

(4) *First month recoverable self-discharge is 5% average.*

(5) *Storage temperature is for uncharged EnerChip.*

Note: All specifications contained within this document are subject to change without notice

EnerChip Discharge Characteristics

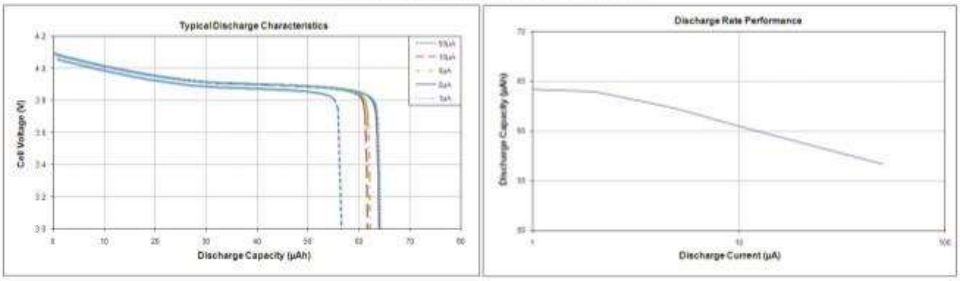

Ordering Information

EnerChip Part Number	Description	Notes
CBC050-M8C	50µAh in 16-pin M8 QFN Package	tube
CBC050-M8C-TR1	50µAh in 16-pin M8 QFN Package	tape & reel 1000 pcs
CBC050-M8C-TR5	50µAh in 16-pin M8 QFN Package	tape & reel 5000 pcs
CBC050-M8C-WP	50µAh in 16-pin M8 QFN Package	waffle pack
CBC050-BDC-WP	50µAh Bare Die	Contact Cymbet
CBC050-BUC-WP	50µAh Bumped Bare Die	Contact Cymbet

Package Dimensions - 16-pin QFN (package code M8)

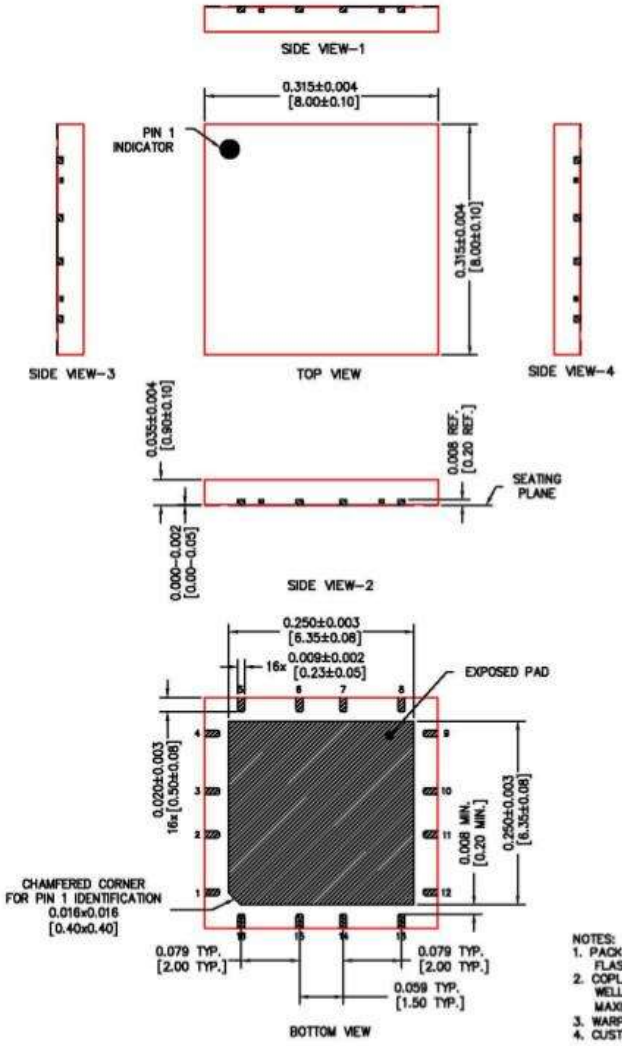

NOTES:
1. PACKAGE DIMENSION DOES NOT INCLUDE MOLD FLASH, PROTRUSIONS, BURRS OR METAL SMEARING.
2. COPLANARITY APPLIES TO THE EXPOSED PAD AS WELL AS THE EXPOSED TERMINALS. MAXIMUM COPLANARITY SHALL BE 0.003 [0.08].
3. WARPAGE SHALL NOT EXCEED 0.004 [0.10].
4. CUSTOM PACKAGE.

[Dimensions in inches [mm]

Printed Circuit Board (PCB) Layout Guidelines and Recommendations

Electrical resistance of solder flux residue on PCBs can be low enough to partially or fully discharge the backup energy cell and in some cases can be comparable to the load typically imposed on the cell when delivering power to an integrated circuit in low power mode. Therefore, solder flux must be thoroughly washed from the board following soldering. The PCB layout can make this problem worse if the cell's positive and negative terminals are routed near each other and under the package, where it is difficult to wash the flux residue away.

To avoid this situation, make sure positive and negative traces are routed outside of the package footprint to ensure that flux residue will not cause a discharge path between the positive and negative pads. Similarly, a leakage current path can exist from the package lead solder pads to the exposed die pad on the underside of the package as well as any solder pad on the PCB that would be connected to that exposed die pad during the reflow solder process. Therefore, it is strongly recommended that the PCB layout not include a solder pad in the region where the exposed die pad of the package will land. It is sufficient to place PCB solder pads only where the package leads will be. That region of the PCB where the exposed die pad will land must not have any solder pads, traces, or vias.

When placing a silk screen on the PCB around the perimeter of the package, place the silk screen outside of the package and all metal pads. Failure to observe this precaution can result in package cracking during solder reflow due to the silk screen material interfering with the solder solidification process during cooling.

A recommended CBC050 PCB layout is shown in Figure 1 below. Notice that there should not be a center pad on the PCB to mate with the exposed die pad on the CBC050 package. Again, this is to reduce the possible number and severity of leakage paths between the EnerChip terminals.

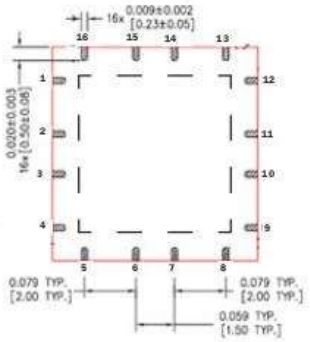

Dimensions in inches [mm]

Figure 1: Recommended PCB layout for the CBC050 package. Do not route signal traces under the EnerChip as they could become shorted to the die pad (as shown by the dotted lines) on the package underside.

Soldering, Rework, and Electrical Test

Refer to the Cymbet User Manual for soldering, rework, and replacement of the EnerChip on printed circuit boards, and for instructions on in-circuit electrical testing of the EnerChip.